Current Research (2009) Newfoundland and Labrador Department of Natural Resources Geological Survey, Report 09-1, pages 13-42

TECTONOSTRATIGRAPHIC ARCHITECTURE AND VMS MINERALIZATION OF THE SOUTHERN TULKS VOLCANIC BELT: NEW INSIGHTS FROM U–Pb GEOCHRONOLOGY AND LITHOGEOCHEMISTRY

J.G. Hinchey and V. McNicoll[1]
Mineral Deposits Section
[1] Geological Survey of Canada, 601 Booth Street, Ottawa, ON, K1A 0E8

ABSTRACT

To clarify their tectonostratigraphic affinity within the Victoria Lake supergroup and to better understand these mineralizing environments, U–Pb geochronology, trace-element lithogeochemistry and Sm/Nd isotopic geochemistry were applied to the host rocks of the Tulks East, Tulks Hill and Boomerang volcanogenic massive sulphide (VMS) deposits, in central Newfoundland.

A subvolcanic porphyry from the Tulks Hill deposit, dated previously at 498 +6/-4 Ma, provides a minimum age for the nearby Tulks Hill and Tulks East deposits. Two, new U–Pb zircon ages were obtained from the felsic tuff that hosts mineralization at the Boomerang deposit and from a felsic dyke interpreted to be broadly synvolcanic. The combined TIMS and SHRIMP data for these two samples indicate an identical U–Pb age of 491 ± 3 Ma. This date is younger than the 498 +6/-4 Ma age from Tulks Hill, although the errors do overlap at their older and younger limits, respectively. Inheritance patterns in the Boomerang samples suggest the presence of older crustal material having Cambrian (514–510 Ma) ages akin to those reported from the Tally Pond group, an older sequence within the Victoria Lake supergroup. The new results suggest that VMS mineralization in the Tulks area and at Boomerang may represent temporally discrete events, despite some apparent similarities. The age determined for the Boomerang deposit is closer to (but not identical with) a U–Pb date of 487 ± 3 Ma, obtained some 30 km to the southwest of the Boomerang deposit, from a unit termed the Pats Pond group. This suggests that the younger sequence of rocks may be regionally extensive, as proposed by other workers, and implies that it may have potential elsewhere for VMS mineralization similar to the Boomerang deposit.

The comparison of lithogeochemical patterns from the Tulks East, Tulks Hill and Boomerang deposit areas, with published data from the Pats Pond group, is complicated by the effects of hydrothermal alteration near the VMS mineralizing environments. Nevertheless, examination of immobile trace-element signatures suggests that these sequences cannot be distinguished on the basis of their geochemistry. The volcanic and pyroclastic rocks are all broadly arc-related, and show a mixture of calc-alkaline and tholeiitic signatures that perhaps record the construction and later rifting of individual arc sequences. However, Nd isotope signatures from felsic rocks in the Boomerang area and the Pats Pond group are higher (εNd of +4 to +5.5) than those from the Tulks Hill and Tulks East areas (εNd of about +3). Although not a straight-forward correlation, as the volcanic rocks that host the Tulks East and Tulks Hill deposits also locally contain higher εNd values of between +4 to +5, the latter observation may also be supportive of a link between the Boomerang area and the Pats Pond group.

Collectively, the new results, when taken with the earlier results, suggest that the tract of rocks known as the Tulks Volcanic Belt includes rocks of more than one age, but of generally similar geochemistry and tectonic setting. There is an immediate need for more geochronological studies and age determinations of other VMS deposits in this area, to ascertain how they might fit into a revised view of this complex but economically important package of rocks.

INTRODUCTION

The Island of Newfoundland boasts numerous volcanogenic massive sulphide (VMS) deposits within Cambrian–Ordovician volcanic arcs and back-arc basins of the Dunnage Zone. The Dunnage Zone is divided by a major suture zone, the Red Indian Line (RIL), into a western terrane representing the Laurentian margin of the ancient Iapetus Ocean and an eastern terrane representing the Gondwanan margin of Iapetus (Williams *et al.*, 1988; Figure 1).

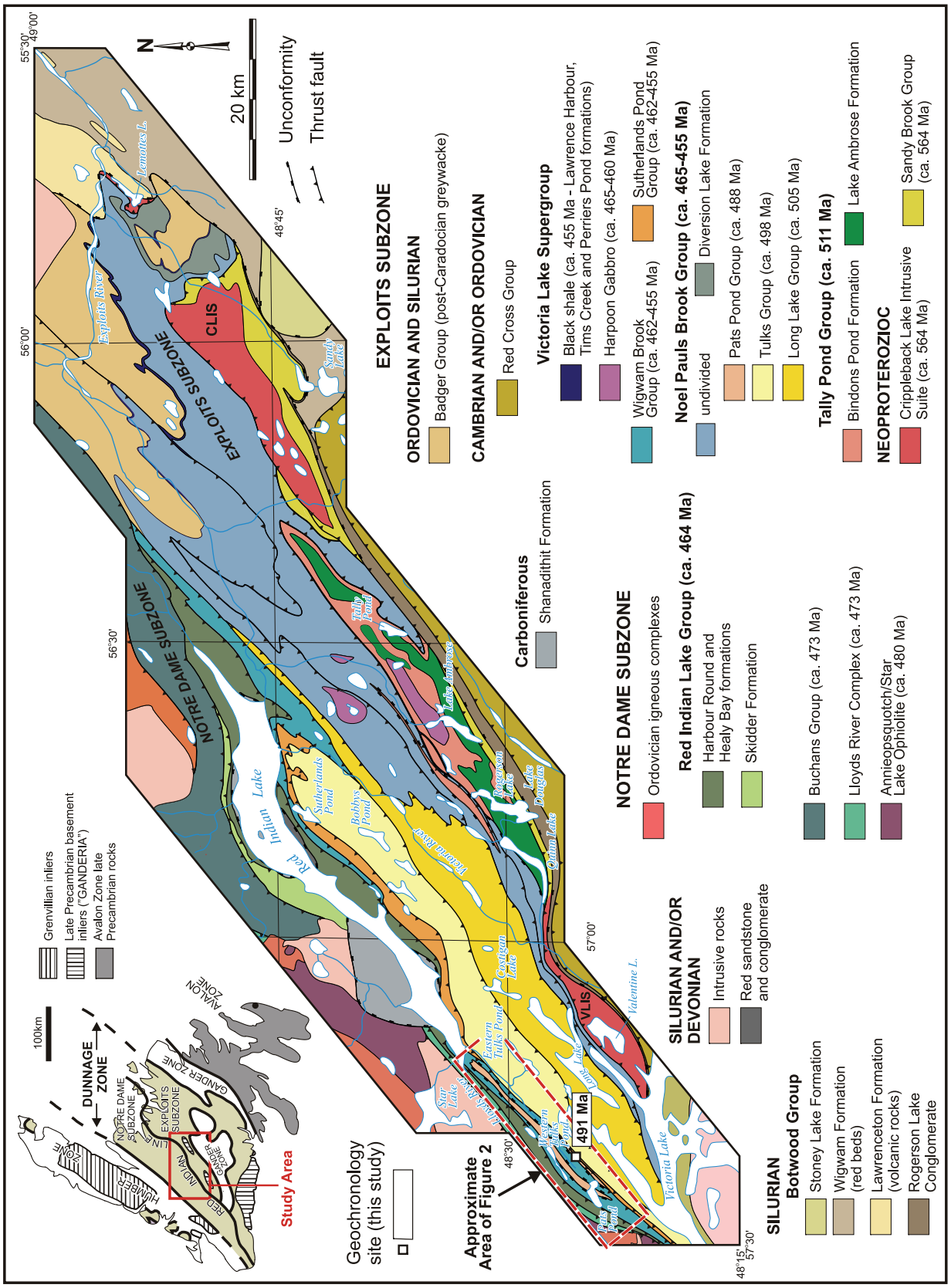

Figure 1. *Location and generalized geology of the area surrounding Red Indian Lake, including rocks of the Victoria Lake supergroup. CLIS - Crippleback Lake intrusive suite; VLIS - Valentine Lake intrusive suite. (Geochronological results from this study are indicated, but others are omitted for the sake of clarity; geological map from a compilation by N. Rogers (GSC), based, in part, on GSC mapping as indicated in the text.)*

The Victoria Lake supergroup (VLSG), located east of the RIL in the Exploits Subzone of the Dunnage Zone, is an important exploration target for VMS deposits. The importance of the VLSG is highlighted by the opening of the Duck Pond mine in 2007 with proven, and probable, reserves of 4.1 Mt containing 3.3% Cu, 5.7% Zn, 62 g/t Ag and 0.85 g/t Au (Aur Resources, press release, May 2007). The 2004 discovery of the Boomerang deposit in the Tulks Volcanic Belt (TVB) of the VLSG, containing an indicated resource of 1.36 Mt, grading 7.09% Zn, 3.00% Pb, 0.51% Cu, 110.43 g/t Ag, and 1.66 g/t Au (Messina Minerals, press release, June 2007), has also generated interest in this part of the study area.

The TVB is bimodal, and is dominated by felsic volcanic rocks containing interbedded mafic volcanic, pyroclastic, volcaniclastic and sedimentary rocks (Evans and Kean, 2002). The age of the TVB was originally constrained by a U–Pb age of 498 +6/-4 Ma on a subvolcanic porphyry near the Tulks Hill VMS deposit (Evans *et al.*, 1990). More recent mapping and compilation by the Geological Survey of Canada, coupled with geochronology and lithogeochemistry (van Staal *et al.*, 2005; Zagorevski *et al.*, 2007a) indicated that the TVB is composite, and also includes sequences of volcanic and sedimentary rocks.

This paper presents and discusses new data from the southern part of the TVB including U–Pb geochronological data obtained from host rocks to the Boomerang VMS deposit. This deposit sits within the originally defined 'Tulks Volcanic Belt', but was placed in the newly defined Pats Pond group, (*ca.* 488 Ma; Zagorevski *et al.*, 2007a; van Staal *et al.,* 2005).

REGIONAL GEOLOGY AND METALLOGENIC FRAMEWORK

The Dunnage Zone of the Newfoundland Appalachians (Figure 1) represents the vestiges of Cambro-Ordovician continental and intra-oceanic arcs, back-arc basins, and ophiolites that formed in the Iapetus Ocean (Kean *et al.*, 1981; Swinden, 1990; Williams, 1995). The zone is bisected by an extensive fault system (the Red Indian Line, RIL) into a western peri-Laurentian segment (Notre Dame and Dashwoods subzones), and an eastern peri-Gondwanan segment (Exploits Subzone). The two main subzones of the Dunnage Zone are differentiated on stratigraphic, structural, faunal, and isotopic characteristics (Williams *et al.*, 1988). The RIL separates the Buchans Group, and locally the Red Indian Lake group (Rogers *et al.*, 2005), which formed on the Laurentian side of the Iapetus Ocean, from the VLSG, that formed on the Gondwanan side of Iapetus. The deformation associated with final closure of the Iapetus Ocean culminated during the Silurian (dated directly as syn- to post- 432 ± 1.4 Ma; Zagorevski *et al.*, 2007b), at which time, thrusting and folding juxtaposed these initially geographically distinct volcanic belts.

Mapping by the Geological Survey of Newfoundland and Labrador (GSNL) in the 1970s and 1980s (*e.g.*, Kean, 1977; Kean *et al.*, 1981; Evans and Kean, 2002 and references therein) indicated that the TVB (*see* Figures 1 and 2) represents the remnants of one of several bimodal Cambrian to Ordovician volcanic-arc sequences. Together with adjacent volcanic and sedimentary belts of variable tectonic affinities, it belongs to the VLSG (Evans and Kean, 2002); subdivided into the TVB (*ca.* 498 Ma), the Long Lake Volcanic/Volcaniclastic Belt (*ca.* 505 Ma), and the Tally Pond Volcanic Belt (*ca.* 515 Ma). In addition to the Cambro-Ordovician volcanic and volcaniclastic rocks of the VLSG, there are also large areas of late Precambrian (565–563 Ma) plutonic rocks (Evans *et al.*, 1990), which represent inliers of old basement, most likely of the crustal block, Ganderia (*e.g.*, van Staal *et al.*, 1998). Previous lithogeochemical studies, based largely on subordinate mafic volcanic rocks, indicate that the VLSG is composed of distinct geochemical groupings representing different tectonic environments, *e.g.*, active arc, arc-rift, back-arc, and mature arc (*see* Swinden *et al.*, 1989; Evans and Kean, 2002).

Evans and Kean (2002) divide the VLSG into the northern and southern terrains, separated by the Rogerson Lake Conglomerate. The TVB, part of the northern terrain, is bounded to the north by the RIL and the sedimentary and volcaniclastic rocks of the Harbour Round Belt (*e.g.*, Red Indian Lake group of Rogers *et al.*, 2005), and to the south by a geophysical anomaly, in the form of a regionally extensive magnetic high, separating the TVB from the Long Lake Belt.

The most common rock types of the southern TVB consist of light grey to white, quartz ± feldspar porphyritic felsic-intermediate pyroclastic rocks, massive rhyolite, and felsic-intermediate ash tuffs through to tuffs and lapilli tuffs, locally bimodal breccias, and minor subvolcanic porphyries. Mafic volcanic rocks are subordinate and are dominated by tuffs, lapilli tuffs, breccias, sills, and locally pillow lavas. Black shales, argillites and greywackes are also locally abundant.

The TVB has been subjected to lower to middle, greenschist-facies metamorphism and moderate to strong deformation. The presence of well-developed, bedding-parallel, regional foliations defined by alignment of chlorite and sericite commonly obliterates primary textures in the rocks. The stratigraphy typically strikes northeast and dips steeply to the northwest, and the belt is transected by shear zones and faults.

All rocks, within the southern part of the TVB, were considered to be of similar age based on a 498 +6/-4 Ma U–Pb date, of a subvolcanic porphyry, located close to the Tulks Hill VMS deposit (Evans *et al.*, 1990). This age was recently re-interpreted by using a weighted average of the $^{207}Pb/^{206}Pb$ ages, versus the original linear regression technique, resulting in a slightly younger age of 496.5 ± 1 Ma (G.R. Dunning, personal communication, 2008).

Recent mapping and geochronological studies by the Geological Survey of Canada (GSC) (Rogers *et al.*, 2005; van Staal *et al.*, 2005) resulted in the interpretation of the southern TVB as a series of generally westward-younging tectonostratigraphic units including the Tulks group (*ca.* 498 Ma), the Pats Pond group (*ca.* 487 Ma), the Sutherlands Pond group (*ca.* 462–457 Ma; Zagorevski *et al.*, 2008, Dunning *et al.*, 1987), and the Wigwam Brook group (*ca.* 453 Ma; van Staal *et al.*, 2005; Zagorevski *et al.*, 2007a). The Wigwam Brook group was dated from a sample of quartz and feldspar phyric tuff immediately south of Pats Pond, but the age of the Pats Pond group was obtained from a sample of bimodal breccia collected in the Burgeo Highway area, approximately 30–35 km southwest of the Boomerang deposit, in a package of rocks physically disconnected from those that host the Boomerang deposit.

PATS POND GROUP

As the Pats Pond group is used throughout this report for comparative purposes with the host rocks to VMS deposits, a brief description of the characteristic rock types is given. As described by Zagorevski *et al.* (2007a), the Pats Pond group is dominated by intermediate quartz-phyric and mafic tuffs. The stratigraphically lowest unit within the group consists of calc-alkaline pillow basalt, overlain by feldspar ± quartz-phyric ash, crystal and lapilli tuffs. These are stratigraphically overlain mainly by quartz-phyric andesitic tuffs, and the stratigraphically highest portion of the group is dominated by basaltic to andesitic tuff, lapilli tuff, and rhyolitic tuff. From the base to the top, Zagorevski (2007a) subdivided the group into six informal geochemical subunits, PP1 through to PP6 (*see* pages 33-36).

VOLCANOGENIC MASSIVE SULPHIDE DEPOSITS

LITHOLOGICAL AND STRATIGRAPHIC SETTING

Massive sulphide deposits in the southern TVB are characteristically associated with felsic-intermediate volcanic rocks (locally quartz ± feldspar, ash-crystal tuffs and rhyolitic flows) hosted within sequences of volcaniclastic and sedimentary rocks containing lesser amounts of mafic volcanic rocks. Abundant bimodal sills are associated with volcaniclastic sedimentary rocks (argillite/wacke) within the mineralized sequences and appear to have been emplaced when the latter were still unconsolidated. This suggests a possible arc-rift or back-arc basin tectonic environment for massive sulphide formation.

From north to south, the three main known VMS deposits in the southern TVB are the Tulks East, the Tulks Hill, and the Boomerang deposits. Mineralization in all three deposits is associated with intense sericite–silica–pyrite, and locally chloritic, alteration and is interpreted to have formed through sub-seafloor replacement processes rather than by exhalative processes (*e.g.,* Squires *et al.*, 2005a,b and Hinchey, 2007).

The Tulks East and Tulks Hill deposits occur within the Jacks Pond formation of the Tulks group (van Staal *et al.*, 2005 and Lissenberg *et al.*, 2005), whereas the Boomerang deposit occurs within the younger Pats Pond group (Zagorevski *et al.*, 2007a and van Staal *et al.*, 2005). These three deposits are evaluated and discussed in terms of their host-rock-types and relationships, geochronology, and lithogeochemical characteristics. For comparative purposes, the lithogeochemistry and geochronology of the Pats Pond group of Zagorevski *et al.* (2007a) will also be examined.

TULKS EAST DEPOSIT

The Tulks East deposit is hosted by a series of sericite–silica–pyrite and, locally, chlorite–carbonate-altered felsic tuffs and lapilli tuffs, quartz-phyric rhyolitic flows and local basaltic sills. Both the hanging wall and footwall of the deposit have undergone hydrothermal alteration and contain stringer-style sulphide mineralization, within an alteration envelope, extending approximately 1600 m along strike, 200 m across strike, and at least 400 m down (McKenzie *et al.*, 1993; Noranda, 1998). The presence of intense hydrothermal alteration and sulphide stringers, in both the hanging wall and footwall stratigraphy, are indicative of a replacement process for mineralization (Hinchey, 2007). Footwall stratigraphy consists mainly of felsic-intermediate ash, crystal (quartz ± feldspar), lapilli tuffs and rhyolitic flows (Plate 1), with minor conglomerate, mafic tuffs, and intermediate to mafic amygdaloidal sills. Mineralization is found toward the top of this stratigraphic package which, in turn, is overlain by a thick sequence of intercalated graphitic argillite, hosting the Tulks East fault, and mafic to intermediate sills and dykes. Hanging-wall rocks, stratigraphically above the graphitic argillite, are dominantly mafic to intermediate sills and lesser amounts of quartz-phyric felsic volcanic rocks.

Petrographically, the quartz-phyric rhyolites display well-preserved textures and contain partially resorbed and

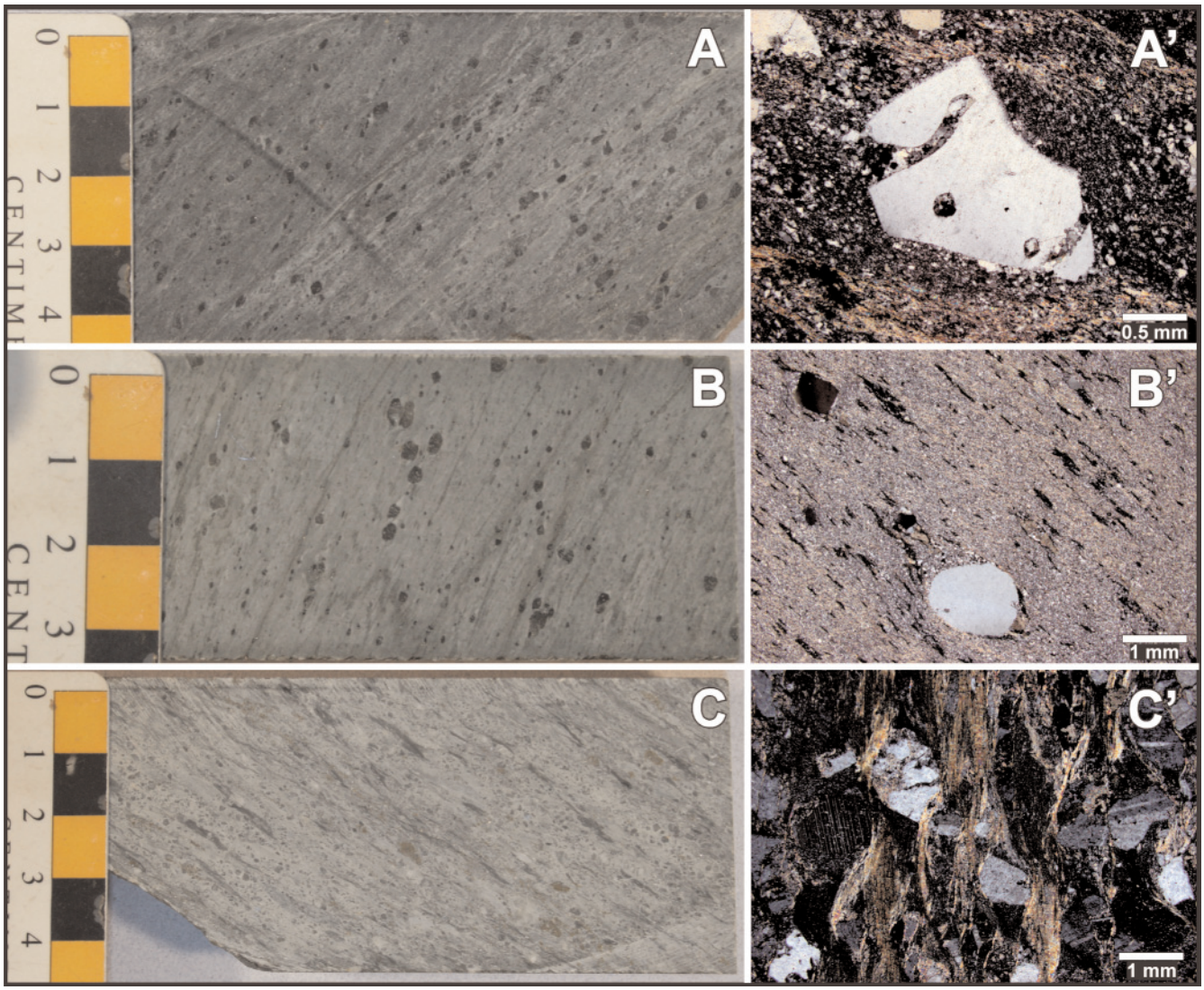

Plate 1. *Macroscopic and microscopic features of the host felsic rocks from the various VMS deposits. (A) Massive and homogenous quartz-phyric rhyolite from the Tulks East deposit. (A') Quartz crystals within a fine-grained recrystallized quartz matrix from a rhyolitic facies at Tulks East deposit. Note the delicate resorption textures occurring as embayments within the quartz crystal, indicative that the quartz phenocrysts were unstable in the melt prior to its solidification. (B) Quartz-phyric rhyolite from the Tulks Hill deposit. (B') Rounded and resorbed quartz phenocrysts within a fine-grained recrystallized quartz and sericite matrix from the Tulks Hill deposit. (C) Quartz- and feldspar-phyric, crystal volcaniclastic tuff from the Boomerang deposit. (C') Quartz and feldspar crystals surrounded by a sericitic matrix from the Boomerang deposit.*

embayed quartz crystals within a fine-grained, recrystallized quartz matrix (Plate 1). The matrix is often partially replaced by sericite. The resorption textures suggest that the quartz phenocrysts, having variably preserved crystals, were unstable in the melt prior to its solidification, being perhaps related to increased temperatures caused by mafic magma influx. In contrast, the felsic tuffaceous rocks contain abundant broken quartz crystals in fine-grained, quartz–sericite matrix.

To date, the Tulks East deposit represents the largest accumulation of sulphide mineralization in the TVB and is distributed in three massive sulphide lenses (termed the A, B, and C zones) totalling about 5.6 Mt (Barbour and Thurlow, 1982). The A-Zone lens is the largest accumulation of sulphide containing about 4.5 Mt of massive sulphide (~ 2% base metals (Zn+Cu+Pb)), but the smaller B-Zone (approximately 0.23 Mt) has higher grades (approximately 8.7% Zn, 0.66% Cu, 1.26% Pb, 58.7 g/t Ag, and 0.14 g/t Au; Barbour and Thurlow, 1982). The C-Zone contains approximately 1 Mt of lower grade, pyritic massive sulphide. The close spatial proximity and overall geological similarities between the Tulks East and Tulks Hill deposits have led to the assumption that both are of the same age.

TULKS HILL DEPOSIT

The Tulks Hill deposit occurs at a similar stratigraphic horizon as the Tulks East deposit, and is hosted by quartz-phyric rhyolite (Plate 1) and altered felsic-intermediate volcanic rocks, dominated by blue quartz ± feldspar-phyric (locally lapilli-rich) tuff. In addition to the felsic-intermediate tuffs and rhyolite, the stratigraphy also contains mafic sills, black argillite and shale, and intermediate volcanic rocks, very similar to those observed at the Tulks East deposit.

The quartz-phyric rhyolites display well-preserved textures and the quartz occurs, both as rounded to teardrop-shaped crystals, in a matrix dominated by fine-grained recrystallized quartz and sericite (Plate 1), to partially resorbed quartz crystals as observed at Tulks East. As at Tulks East, the felsic tuffaceous rocks contain abundant broken quartz crystals in fine-grained, quartz-sericite matrix.

Prominent sericite, chlorite, pyrite and silica alteration is observed within the host felsic quartz-eye tuff and quartz-phyric rhyolite in proximity to the sulphide lenses. These features, along with alteration and related stringer mineralization present, in both the hanging wall and footwall, are indicative of a replacement process for mineralization (Kean and Evans, 1986). Alteration associated with the sulphide lenses has been observed over a 2000-m-long zone (McKenzie *et al.*, 1993).

The deposit consists of four tabular massive sulphide lenses (T1 to T4) collectively containing 720 000 tonnes of massive sulphide, grading 5.6% Zn, 1.3% Cu, 2.0% Pb, 41 g/t silver and 0.4 g/t gold (Jambor and Barbour, 1987). Lenses T1, T2 and T3 outcrop on surface and are marked by heavily gossaned areas, whereas the T4 lense occurs at depth. Isoclinal folding in the area suggests that some of the lenses may represent structural repetitions of the same horizons (Moreton, 1984; Saunders, 1999). In addition to pyrite and base metals, significant magnetite also occurs within the T1 and T2 lenses and serves to discriminate the ore from other massive-sulphide bodies in the area. The significance, if any, of the magnetite is unknown.

BOOMERANG DEPOSIT AND RELATED ZONES

The Boomerang, Domino and Hurricane VMS deposits are located in the southern portion of the TVB in the vicinity of Pats Pond, approximately 17.5 km southwest of the southern tip of Red Indian Lake (Figures 1 and 2). For the purposes of this report, all of the massive sulphide lenses will be grouped together under the name 'Boomerang' to simplify discussion.

The Boomerang deposit stratigraphy consists of a series of felsic-intermediate volcanic rocks including quartz±feldspar phyric ash-crystal tuffs (Plate 1), lapilli tuffs, coarse-grained volcaniclastic rocks (conglomerate and breccia), sedimentary rocks (black argillite, siltstone, chert and black shales), felsic, intermediate and amygdaloidal mafic sills, and intermediate dykes. The rocks are dominated by volcaniclastic material, with a general lack of massive, coherent rhyolite, which contrasts with the local abundance of the latter at the Tulks Hill and Tulks East deposits.

Based on observed inter-fingering and 'soft-sediment' intrusive textures, the bimodal sills are considered to be synchronous with the volcanic and sedimentary rocks in the stratigraphy, an observation substantiated by geochronology (*see* below, pages 20-24). Well-defined fining-upward sedimentary sequences (*e.g.*, turbiditic sequences) are commonly observed in drillcore, and along with the bimodal sills may indicate an arc-rift type environment. All rock types, with the exception of some of the late sills, are overprinted by strong northwest-dipping foliations. The observation that some sills are foliated whereas others are massive with little to no foliation suggests possible different ages for various sills, or competency contrasts.

The deposit's stratigraphy is divided into a hanging-wall sequence, a mineralized horizon, and a footwall sequence (*see* Squires *et al.*, 2006; Dearin, 2006). The hanging wall sequence consists of undifferentiated, locally fining-upward, felsic-intermediate volcanic rocks dominated by quartz±feldspar crystal-ash tuffs, fine-grained sedimentary rocks (black shales/argillite/greywacke/chert), volcaniclastic conglomerate/breccia, and bimodal sills. Footwall rocks consist of strongly sericitized felsic-intermediate volcanic rocks (dominated by fine-grained, pyroclastic crystal-ash tuffs) that commonly contain base-metal stringer sulphides. The rocks are extremely sericitized and display an intense foliation and a local crenulation cleavage. The mineralized horizon of the Boomerang deposit consists of strongly altered, fine-grained pyroclastic felsic-intermediate volcanic rocks (ash-crystal tuffs) and sedimentary rocks (black shales, chert and argillite) that are intimately associated with massive sulphide mineralization. The intercalation of volcanic, pyroclastic and sedimentary rocks provided a favourable environment for the formation of the Boomerang massive sulphide lense *via* replacement (*see* Hinchey, 2007; Squires, 2008; Squires *et al.*, 2005).

The dominant quartz–feldspar–phyric, felsic-intermediate tuff consists of abundant, variably preserved, quartz and feldspar crystals in an intermediate fine-grained groundmass, commonly altered to sericite (Plate 1). All textures at the Boomerang deposit are indicative of volcaniclastic

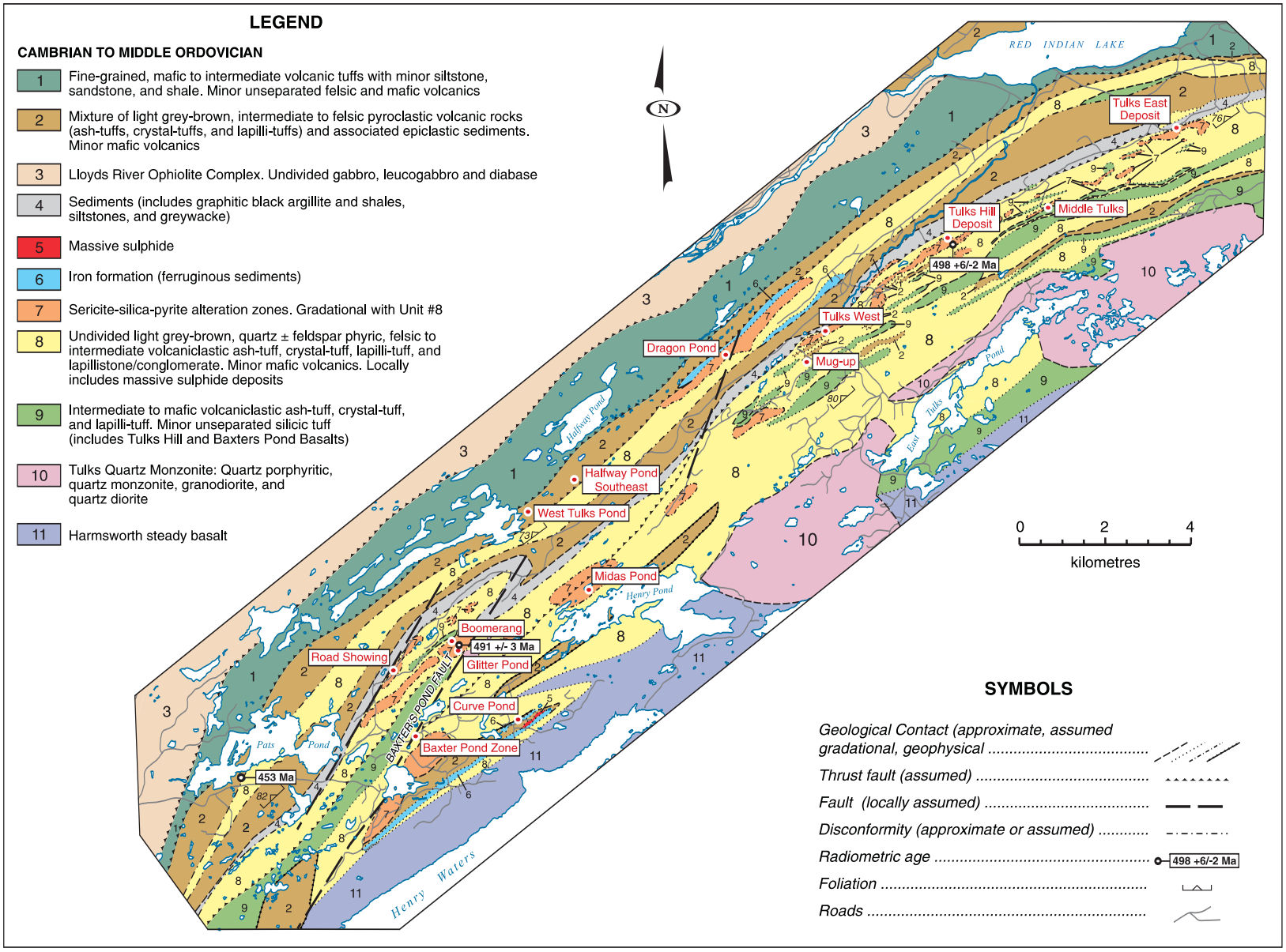

Figure 2. *Geology map of the southern Tulks Volcanic Belt illustrating the various rock types and the VMS deposits, prospects, and showings. Note that the map is not intended to distinguish the various groupings defined by van Staal et al. (2005), but is rather meant to represent a lithological map. (Partly modified and compiled from industry sources (*e.g.*, Noranda, 1998) and government publications (*e.g.*, Kean, 1982; Evans* et al.*, 1994; Evans and Kean, 2002; van Staal* et al.*, 2005)).*

facies compared to the more coherent facies observed in the Tulks East and Tulks Hill deposits.

Hydrothermal alteration, predominantly sericite–silica–pyrite along with local chlorite and carbonate, and stringer base-metal sulphides, occur in both the hanging wall and footwall of the massive sulphide lense, although the alteration is much more intense in the footwall rocks. The deposit displays metal zonations with a Cu- and Zn-enriched bottom and a gold-enriched top. A recent NI43-101 compliant mineral resource estimate for the Boomerang lense returned an indicated resource of 1.36 Mt grading 7.09% Zn, 3.00% Pb, 0.51% Cu, 110.43 g/t Ag, and 1.66 g/t Au (Messina Minerals Inc., press release, June 21, 2007). An additional 0.7 Mt of inferred resources is estimated for the Boomerang and Domino lenses. In contrast to the medium- to coarse-grained, massive sulphides associated with the Tulks Hill and Tulks East deposits, the sulphides in the Boomerang deposit are dominated by fine- to medium-grained, banded and wispy, sphalerite–galena–chalcopyrite–pyrite intergrowths.

U–Pb GEOCHRONOLOGY

Geochronological studies were initiated in an attempt to further characterize the stratigraphy of the southern TVB and constrain the timing of VMS mineralization. The data below summarize results of U–Pb TIMS and SHRIMP geochronology from the host rocks of the Boomerang deposit. The U–Pb geochronology analysis was done at the Geochronology Laboratory, of the Geological Survey of Canada, as part of a collaborative study with the GSC.

ANALYTICAL METHODS

The geochronology samples were collected from drill-core. Heavy mineral concentrates were prepared by standard crushing, grinding, Wilfley table, and heavy liquid separation techniques. Mineral separates were sorted by magnetic susceptibility using a Frantz™ isodynamic separator.

The U–Pb isotope dilution-thermal ionization mass spectrometer (ID-TIMS) analytical methods utilized in this study are outlined in Parrish *et al.* (1987). Multigrain zircon fractions for TIMS analyses comprised between 10 to 25 grains (*see* Table 1) and were very strongly air abraded following the method of Krogh (1982). Details of zircon morphology and quality are summarized in Table 1. Treatment of analytical errors follows Roddick (1987), with regression analysis modified after York (1969). The U–Pb TIMS analytical results are presented in Table 1, where errors on the ages are reported at the 2σ level, and displayed in a concordia plot (Figure 3a).

Table 1. U–Pb TIMS analytical data

Fract.[1]	Description[2]	Wt.	U	Pb[3]	$^{206}Pb/^{204}Pb$[4]	Pb[5]	$^{208}Pb/^{206}Pb$	Isotopic Ratios[6] $^{207}Pb/^{235}U$	±1SE Abs	$^{206}Pb/^{238}U$	±1SE Abs	Corr.[7] Coeff.	$^{207}Pb/^{206}Pb$	±1SE Abs	$^{206}Pb/^{238}U$	±2SE	Ages (Ma)[8] $^{207}Pb/^{235}U$	±2SE	$^{207}Pb/^{206}Pb$	±2SE	% Disc
		ug	ppm	ppm		pg															
JHC-06-239 (z9127): Ash/lapilli tuff, Boomerang deposit																					
A1 (Z;21)	Co,Clr,fIn,fFr,Eu,El, Dia	30	36	3	106	63	0.21	0.70382	0.01320	0.08164	0.00042	0.700	0.06253	0.00097	505.9	5.0	541.1	15.7	692.1	65.1	28.0
A2 (Z;20)	Co,Clr,fIn,fFr,Eu,El, Dia	40	57	5	407	29	0.19	0.62881	0.00278	0.07946	0.00012	0.698	0.05739	0.00020	492.9	1.5	495.4	3.5	506.7	15.4	2.8
A3 (Z;21)	Co,Clr,fIn,fFr,Eu,El, Dia	41	81	7	372	47	0.18	0.63199	0.00312	0.07989	0.00013	0.709	0.05738	0.00023	495.5	1.6	497.3	3.9	506.0	17.3	2.2
B1 (Z;19)	Br,Clr,fIn,fFr,Eu,Pr,Dia	33	59	5	400	25	0.19	0.62987	0.00285	0.07949	0.00013	0.700	0.05747	0.00021	493.1	1.5	496.0	3.6	509.6	15.7	3.4
B2 (Z;25)	Co,Clr,fIn,fFr,Eu,Pr,Dia	40	83	7	253	70	0.18	0.63532	0.00430	0.07980	0.00017	0.702	0.05774	0.00032	494.9	2.0	499.4	5.3	520.0	23.9	5.0
C1 (Z;10)	Br,Clr,fIn,fFr,Eu,St,Dia	33	64	5	673	16	0.18	0.63209	0.00179	0.07932	0.00011	0.686	0.05779	0.00012	492.1	1.3	497.4	2.2	521.9	9.4	5.9
C2 (Z;15)	Co.Clr,fIn,fFr,Eu,St,Dia	60	99	8	266	12	0.17	0.66413	0.00690	0.07993	0.00017	0.530	0.06026	0.00057	495.7	2.0	517.1	8.4	612.9	40.2	19.9

Notes:
[1]Z=zircon. Number in bracket refers to the number of grains in the analysis.
[2]Fraction descriptions: Br=Light Brown, Co=Colourless, Clr=Clear, fFr=Few Fractures, fIn=Few Inclusions, Eu=Euhedral, El=Elongate, Pr=Prismatic, St=Stubby Prism, Dia=Diamagnetic.
[3]Radiogenic Pb
[4]Measured ratio, corrected for spike and fractionation
[5]Total common Pb in analysis corrected for fractionation and spike
[6]Corrected for blank Pb and U and common Pb, errors quoted are 1 sigma absolute; procedural blank values for this study ranged from <0.1- 0.1 pg for U and 1-3 pg for Pb; Pb blank isotopic composition is based on the analysis of procedural blanks; corrections for common Pb were made using Stacey-Kramers compositions
[7]Correlation coefficient
[8]Corrected for blank and common Pb, errors quoted are 2 sigma in Ma

The Sensitive High Resolution Ion MicroProbe (SHRIMP II) analyses were conducted using analytical and data reduction procedures described by Stern (1997) and Stern and Amelin (2003). Zircons from the samples and fragments of the GSC laboratory zircon standard (z6266 zircon, with $^{238}U/^{206}Pb$ age = 559 Ma) were cast in an epoxy grain mount (mount IP419), polished with diamond compound to reveal the grain centres, and photographed in transmitted light. The mount was evaporatively coated with 10 nm of high purity Au, and the internal features of the zircons were characterized with backscattered electrons (BSE) utilizing a scanning electron microscope (SEM). Analyses were conducted using an O^- primary beam projected onto the zircons with an elliptical spot size of 25 μm (in the longest dimension). The count rates of ten isotopes of Zr^+, U^+, Th^+, and Pb^+ in zircon were sequentially measured using a single electron multiplier. Off-line data processing was accomplished using customized in-house software. The SHRIMP analytical data is presented in Table 2. Common Pb-corrected ratios and ages are reported with 1σ analytical error, which incorporate an external uncertainty of 1.1% in calibrating the standard zircon (*see* Stern and Amelin, 2003). The $^{238}U/^{206}Pb$ ages for the analyses have been corrected for common Pb using both the 204- and 207-methods (Stern, 1997), but there is no significant difference in the results.

The data are plotted in concordia diagrams with errors at the 2σ level (Figures 3b and 3c), using Isoplot v. 3.0 (Ludwig, 2003) to generate the plots. A Concordia age (Ludwig, 1998) is calculated for some of the samples presented. A Concordia age incorporates errors on the decay constants and includes both an evaluation of concordance and an evaluation of equivalence of the data. The calculated Concordia age and errors quoted in the text are at 2σ with decay constant errors included.

RESULTS

Sample JHC-06-239 (z9127)

A sample of intermediate ash to lapilli tuff was collected from diamond-drill core, Hole GA-05-016 (interval 345.7–360.1 m). The sample sits directly above the massive sulphide zone at the Boomerang deposit. The sulphide in the deposit replaces this same rock type (Squires *et al.*, 2005; Hinchey, 2007) suggesting that the rock was not completely consolidated during the time of the mineralizing processes, and, as such, the age is interpreted as being syn-mineralization.

The sample yielded abundant zircon of fairly good quality, and only minor fractures and inclusions were present in almost all of the grains; zircon morphology ranges from stubby prismatic to elongate. Multigrain zircon fractions were analyzed by ID-TIMS. These data, which were

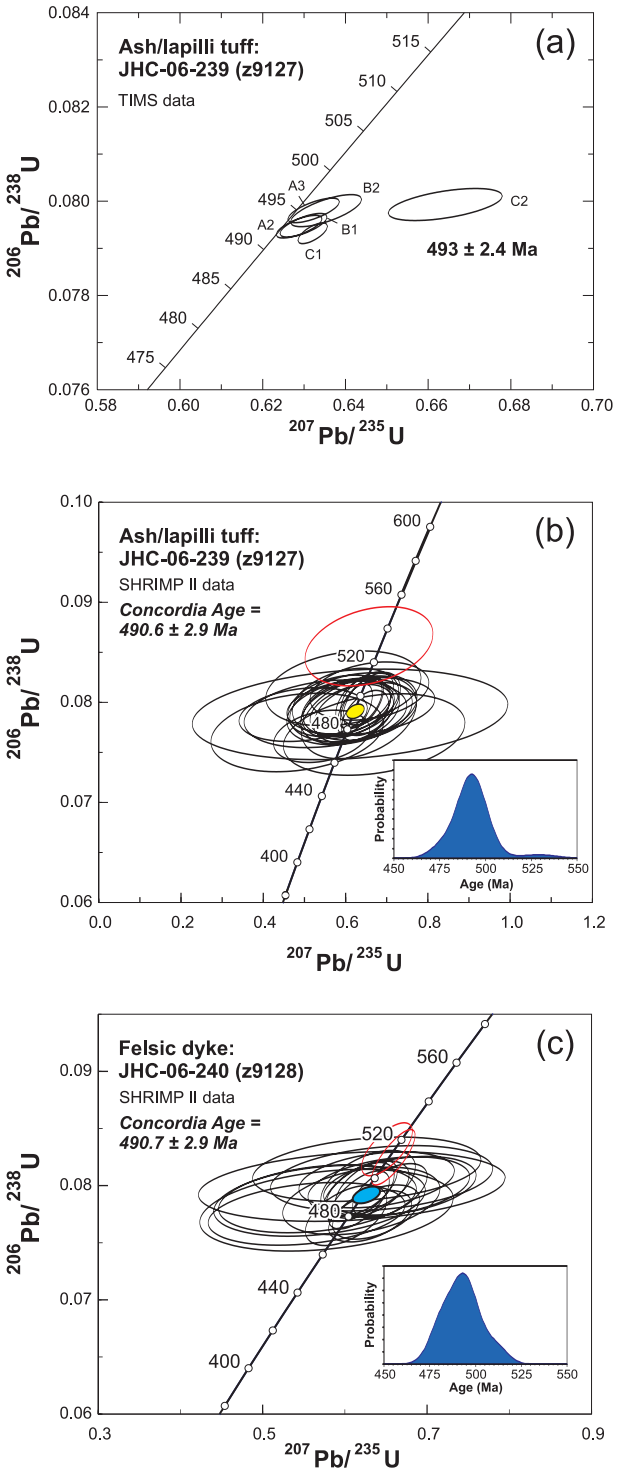

Figure 3. *a) U–Pb concordia diagram for the ash/lapilli tuff from the Boomerang deposit; analyzed using ID-TIMS techniques, b) U–Pb concordia diagram for the ash/lapilli tuff from the Boomerang deposit; analyzed using SHRIMP II techniques. A cumulative probability plot of the data is inset, c) U–Pb concordia diagram for the felsic dyke from the Boomerang deposit; analyzed using SHRIMP II techniques. A cumulative probability plot of the data is inset.*

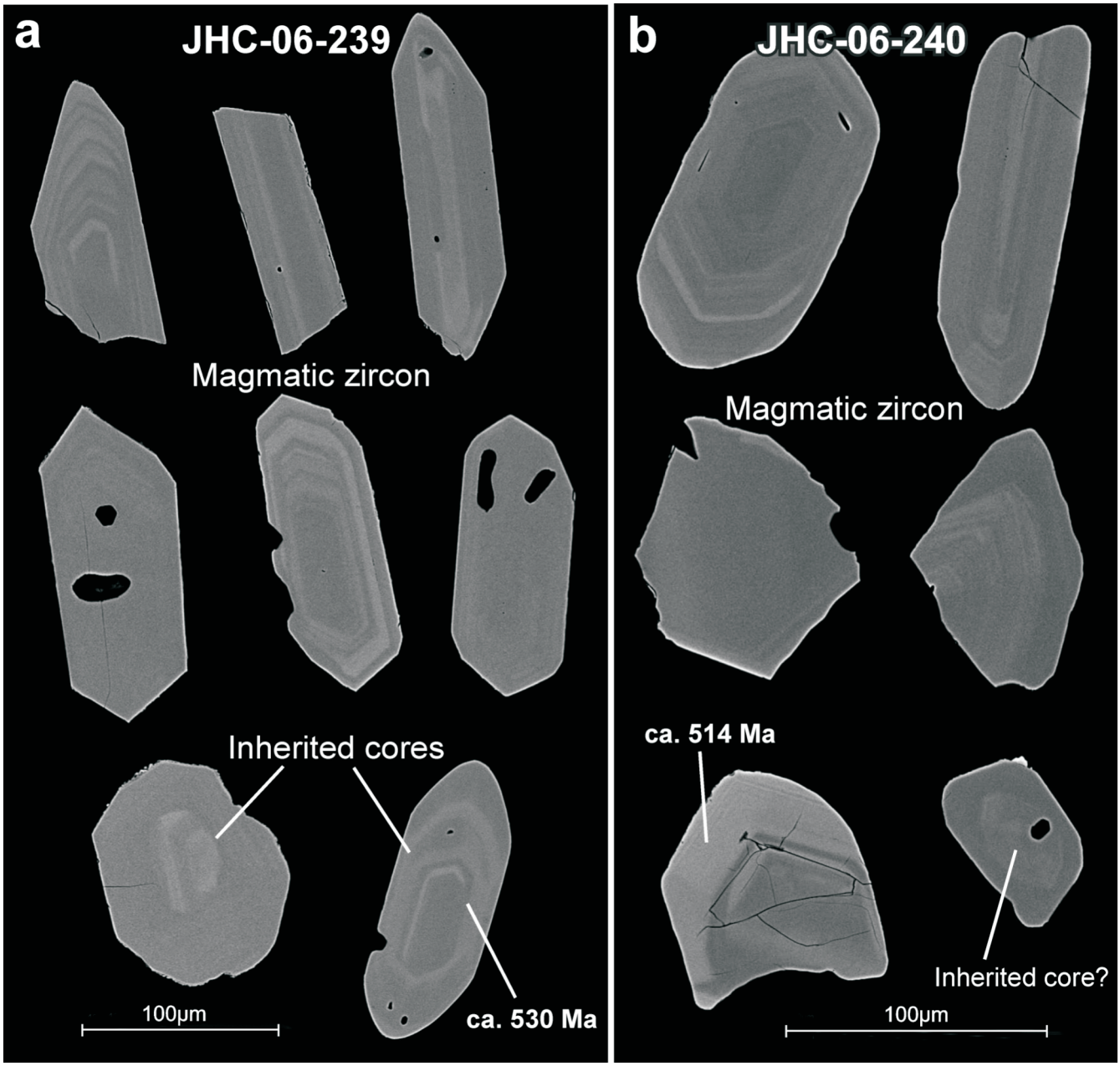

Plate 2. *Representative back-scattered electron images of zircons from: a) felsic ash – lapilli tuff from the Boomerang deposit and b) felsic dyke from the Boomerang deposit.*

analyzed in four different U–Pb chemistry batches, contain a significant amount of common lead (12–70 pg, Table 1), which is related to the inclusions present in most of the zircon, as opposed to procedural lead blanks. Some of the zircon analyses are quite discordant (20–28%) and contain inherited components (C2 and A1, not plotted); however, some of the fractions are nearly concordant (Figure 3a; Table 1). A weighted average of the $^{238}U/^{206}Pb$ ages of the most concordant analyses is calculated to be 493.0 ± 2.4 Ma (MSWD=1.8). There is some scatter of the data, which is most likely a result of minor inheritance in these analyses.

Representative zircons from the sample were placed on a grain mount for imaging with a backscatter detector on a scanning electron microscope. Many of the zircons are interpreted as magmatic having well-defined oscillatory zoning (Plate 2a). Other grains appear to contain inherited cores and show good core-rim relationships.

The SHRIMP data for this sample define a cluster overlapping concordia (Figure 3b; Table 2). A Concordia age is calculated to be 490.6 ± 2.9 Ma (MSWD of concordance and equivalence = 0.72; probability = 0.95; n=22). This cal-

Table 2. U/Pb SHRIMP analytical data

Spot name	U (ppm)	Th (ppm)	Th/U	Pb* (ppm)	^{204}Pb (ppb)	^{204}Pb/^{206}Pb	± ^{204}Pb/^{206}Pb	f(206)^{204}	^{208}Pb/^{206}Pb	± ^{208}Pb/^{206}Pb	^{207}Pb/^{235}U	±^{207}Pb/^{235}U	^{206}Pb/^{238}U	±^{206}Pb/^{238}U	Corr Coeff	^{207}Pb/^{206}Pb	±^{207}Pb/^{206}Pb	Ages (Ma) ^{206}Pb/^{238}U	±^{206}Pb/^{238}U	^{207}Pb/^{206}Pb	±^{207}Pb/^{206}Pb
JHC-06-239 (z9127): Ash/lapilli tuff, Boomerang deposit																					
9127-1.1	108	43	0.410	9	2	0.000248	0.000269	0.0043	0.1255	0.0117	0.5851	0.0515	0.0796	0.0013	0.298	0.0533	0.0045	494	7	341	204
9127-2.1	105	44	0.435	9	1	0.000101	0.000225	0.0018	0.1311	0.0130	0.6021	0.0441	0.0794	0.0012	0.327	0.0550	0.0038	492	7	413	164
9127-3.1	109	46	0.438	9	0	0.000010	0.000010	0.0002	0.1409	0.0065	0.6436	0.0200	0.0800	0.0010	0.524	0.0584	0.0016	496	6	544	59
9127-4.1	142	87	0.636	12	3	0.000303	0.000220	0.0052	0.1850	0.0122	0.6078	0.0454	0.0794	0.0012	0.313	0.0555	0.0040	492	7	434	168
9127-6.1	64	35	0.560	5	1	0.000296	0.000429	0.0051	0.1637	0.0180	0.5512	0.0808	0.0788	0.0014	0.241	0.0507	0.0073	489	8	227	301
9127-7.1	134	59	0.456	11	0	0.000010	0.000010	0.0002	0.1609	0.0058	0.6229	0.0175	0.0793	0.0010	0.566	0.0570	0.0013	492	6	491	52
9127-8.1	55	23	0.421	4	0	0.000010	0.000010	0.0002	0.1420	0.0084	0.6326	0.0573	0.0785	0.0017	0.354	0.0585	0.0050	487	10	548	198
9127-9.1	88	49	0.576	7	2	0.000341	0.000248	0.0059	0.1519	0.0181	0.6113	0.0489	0.0790	0.0013	0.322	0.0562	0.0043	490	8	458	179
9127-10.1	122	57	0.484	9	4	0.000494	0.000254	0.0086	0.1313	0.0110	0.5426	0.0478	0.0766	0.0011	0.278	0.0514	0.0044	476	6	258	209
9127-11.1	70	27	0.395	5	3	0.000612	0.000344	0.0106	0.1108	0.0197	0.5747	0.0624	0.0767	0.0012	0.269	0.0544	0.0057	476	7	387	256
9127-12.1	178	88	0.508	15	0	0.000010	0.000010	0.0002	0.1639	0.0050	0.6329	0.0232	0.0800	0.0011	0.470	0.0574	0.0019	496	6	507	73
9127-13.1	98	59	0.626	8	7	0.001009	0.000352	0.0175	0.1630	0.0162	0.4974	0.0638	0.0788	0.0011	0.231	0.0458	0.0058	489	7	0	0
9127-14.1	177	110	0.642	15	0	0.000015	0.000286	0.0003	0.1950	0.0120	0.6436	0.0529	0.0791	0.0012	0.301	0.0590	0.0047	490	7	569	182
9127-15.1	170	116	0.705	15	0	0.000010	0.000010	0.0002	0.2074	0.0066	0.6532	0.0263	0.0804	0.0011	0.444	0.0590	0.0021	498	6	566	81
9127-18.1	73	42	0.597	6	0	0.000010	0.000010	0.0002	0.2046	0.0161	0.6479	0.0232	0.0786	0.0010	0.481	0.0598	0.0019	488	6	595	70
9127-19.1	51	22	0.442	4	0	0.000010	0.000010	0.0002	0.1473	0.0104	0.6605	0.0296	0.0798	0.0013	0.472	0.0600	0.0024	495	8	604	89
9127-20.1	95	35	0.378	8	1	0.000118	0.000362	0.0021	0.1231	0.0159	0.6373	0.0738	0.0796	0.0012	0.247	0.0581	0.0066	494	7	532	269
9127-21.1	102	44	0.450	8	0	0.000050	0.000340	0.0009	0.1408	0.0141	0.6196	0.0631	0.0795	0.0014	0.294	0.0565	0.0056	493	8	474	233
9127-22.1	162	104	0.660	14	3	0.000225	0.000278	0.0039	0.1976	0.0122	0.6005	0.0531	0.0801	0.0013	0.310	0.0544	0.0046	497	8	387	202
9127-23.1	129	51	0.411	11	3	0.000286	0.000252	0.0050	0.1272	0.0110	0.6584	0.0591	0.0811	0.0012	0.284	0.0589	0.0051	503	7	563	201
9127-63.1	146	56	0.394	12	0	0.000031	0.000182	0.0005	0.1189	0.0131	0.6201	0.0393	0.0789	0.0012	0.356	0.0570	0.0034	489	7	493	137
9127-65.1	195	130	0.685	17	3	0.000262	0.000337	0.0046	0.2050	0.0147	0.6094	0.0623	0.0790	0.0013	0.286	0.0559	0.0055	490	8	449	236
9127-25.1	104	65	0.645	10	1	0.000186	0.000275	0.0032	0.1890	0.0125	0.6578	0.0635	0.0856	0.0016	0.315	0.0558	0.0052	529	10	443	220
JHC-06-240 (z9128): Felsic dyke, Boomerang deposit																					
9128-8.1	225	121	0.557	19	0	0.000010	0.000010	0.0002	0.1708	0.0046	0.6261	0.0155	0.0798	0.0010	0.588	0.0569	0.0012	495	6	489	45
9128-9.1	222	123	0.572	18	0	0.000010	0.000010	0.0002	0.1759	0.0067	0.6307	0.0205	0.0772	0.0009	0.475	0.0592	0.0017	480	5	575	64
9128-2.1	229	108	0.487	19	0	0.000010	0.000010	0.0002	0.1583	0.0099	0.6381	0.0216	0.0776	0.0010	0.481	0.0596	0.0018	482	6	590	66
9128-3.1	125	54	0.445	10	3	0.000359	0.000268	0.0062	0.1242	0.0113	0.5538	0.0490	0.0775	0.0011	0.285	0.0519	0.0044	481	7	279	208
9128-4.1	162	71	0.455	13	0	0.000010	0.000010	0.0002	0.1388	0.0051	0.6169	0.0178	0.0794	0.0011	0.566	0.0564	0.0014	492	6	467	54
9128-5.1	137	63	0.474	11	0	0.000010	0.000010	0.0002	0.1514	0.0060	0.6279	0.0206	0.0796	0.0010	0.499	0.0572	0.0016	494	6	500	64
9128-6.1	262	160	0.632	23	1	0.000063	0.000163	0.0011	0.1989	0.0077	0.6389	0.0387	0.0804	0.0010	0.324	0.0576	0.0033	499	6	515	132
9128-10.1	181	103	0.590	15	2	0.000197	0.000392	0.0034	0.1747	0.0165	0.6083	0.0762	0.0798	0.0012	0.246	0.0553	0.0068	495	7	423	299
9128-11.1	290	139	0.494	24	0	0.000010	0.000010	0.0002	0.1527	0.0041	0.6171	0.0151	0.0787	0.0010	0.637	0.0569	0.0011	488	6	487	43
9128-12.1	131	66	0.520	11	0	0.000019	0.000288	0.0003	0.1579	0.0136	0.6447	0.0553	0.0806	0.0012	0.289	0.0581	0.0048	499	7	532	192
9128-13.1	156	68	0.447	12	2	0.000184	0.000176	0.0032	0.1227	0.0102	0.5667	0.0492	0.0788	0.0012	0.297	0.0522	0.0044	489	7	294	203
9128-14.1	136	69	0.524	11	1	0.000120	0.000195	0.0021	0.1533	0.0149	0.6205	0.0391	0.0786	0.0012	0.360	0.0573	0.0034	488	7	502	136
9128-15.1	161	74	0.472	13	0	0.000010	0.000010	0.0002	0.1505	0.0122	0.6552	0.0185	0.0795	0.0010	0.539	0.0598	0.0014	493	6	596	53
9128-17.1	123	56	0.470	10	0	0.000010	0.000010	0.0002	0.1502	0.0081	0.6285	0.0235	0.0801	0.0012	0.498	0.0569	0.0019	497	7	487	74
9128-7.1	298	153	0.529	24	2	0.000095	0.000077	0.0017	0.1587	0.0048	0.6019	0.0202	0.0773	0.0011	0.519	0.0565	0.0016	480	6	470	65
9128-19.1	190	118	0.640	16	1	0.000055	0.000187	0.0010	0.2020	0.0089	0.6537	0.0402	0.0798	0.0011	0.334	0.0594	0.0035	495	6	581	132
9128-3.2	178	79	0.457	14	7	0.000550	0.000279	0.0095	0.1341	0.0126	0.5693	0.0525	0.0786	0.0013	0.294	0.0525	0.0047	488	8	308	216
9128-4.2	408	216	0.546	35	8	0.000290	0.000309	0.0050	0.1588	0.0126	0.6270	0.0567	0.0814	0.0011	0.276	0.0559	0.0049	504	7	449	208
9128-6.2	247	191	0.798	21	9	0.000535	0.000352	0.0093	0.2235	0.0180	0.5780	0.0631	0.0778	0.0015	0.293	0.0539	0.0057	483	9	367	256
9128-8.2	217	143	0.682	19	1	0.000053	0.000170	0.0009	0.2144	0.0094	0.6671	0.0380	0.0799	0.0010	0.347	0.0606	0.0033	496	6	623	120
9128-16.1	968	625	0.667	87	0	0.000006	0.000018	0.0001	0.2068	0.0024	0.6572	0.0108	0.0823	0.0010	0.798	0.0579	0.0006	510	6	527	22
9128-18.1	1204	1015	0.871	113	1	0.000010	0.000010	0.0002	0.2589	0.0056	0.6495	0.0126	0.0830	0.0009	0.676	0.0568	0.0008	514	6	482	32

Notes (see Stern, 1997):
Uncertainties reported at 1s (absolute) and are calculated by numerical propagation of all known sources of error
f206^{204} refers to mole fraction of total ^{206}Pb that is due to common Pb, calculated using the ^{204}Pb-method; common Pb composition used is the surface blank

culation utilized all of the SHRIMP analyses except one that is highlighted in red on Figure 3b. This older analysis at *ca.* 530 Ma (Table 2) is interpreted to be from an inherited zircon. The date of 491 ± 3 Ma is taken to be the crystallization age of the zircon in the tuff and constrains the timing of mineralization. Although the sulphides have replaced this host rock, the interval between deposition and mineralization is not considered significant (*e.g.*, *see* Hinchey, 2007).

Sample JHC-06-240 (z9128)

A sample of a felsic dyke was collected from diamond-drill core, Hole GA-05-079 (interval 247.1–264.0 m), directly above the sulphide zone at the Boomerang deposit. The sample yielded a very small amount of zircon; not enough material for ID-TIMS analysis, so the zircon retrieved was placed on a grain mount and analyzed using the SHRIMP. Backscatter SEM images reveal oscillatory-zoned grains that appear magmatic and also grains with possible inherited cores (Plate 2b).

The SHRIMP data define a cluster of data overlapping concordia (Figure 3c; Table 2). A Concordia age, utilizing all of the SHRIMP analyses except 2 outlined below, is calculated to be 490.7 ± 2.9 Ma (MSWD of concordance and equivalence = 0.96; probability = 0.54; n=20). This date of 491 ± 3 Ma is interpreted to be the crystallization age of the felsic dyke and it suggests that the dyke is synchronous with the tuffaceous rocks represented by sample JHC-06-239 (z9127).

Two of the analyses are slightly older with ages of *ca.* 510 and 514 Ma (Table 2; highlighted in red on Figure 3c). These zircons are interpreted to be entirely inherited grains in the rock. These inheritance ages are the same as the crystallization ages of volcanic rocks previously dated at the Duck Pond deposit (McNicoll *et al.*, 2008). As the zircon yield was poor in the sample from this study, there is the possibility that all of the zircon in the felsic dyke is xenocrystic, *i.e.*, inherited from the rocks that the dyke has intruded.

GEOCHEMISTRY

A representative suite of all volcanic and volcaniclastic rock types from the TVB was analyzed for major and trace elements using Inductively Coupled Plasma – Emission Spectrometry (ICP-ES) methods outlined in Finch (1998). A smaller subset of samples was analyzed at Acme Analytical Laboratories for trace elements and rare-earth elements (REE) by four-acid digestion, Inductively Coupled Plasma – Mass Spectrometry (ICP-MS) techniques. Samples were separated into groups based upon their association with the specific VMS deposits described above and, where possible, were further divided into hanging wall and footwall categories to aid in identifying the affects of alteration. Selected samples were also analyzed for Sm/Nd isotopic compositions (Table 3) by Thermal Ionization Mass Spectrometry (TIMS) techniques at Memorial University. The complete geochemical database derived from this project will be released later, when the project is completed. Selected chemical ratios for various rock types from each deposit are listed in Table 3 to aid in discussion and comparison.

The samples analyzed in this study cover all rock types and include both altered and unaltered samples. It is very difficult to obtain unaltered material for geochemical analyses, because outcrop is limited, and exploration is naturally focused around areas of mineralization. Most of the samples represent drillcore.

ELEMENT MOBILITY CONSIDERATIONS

It is important to account for the effects of element mobility, especially if using lithogeochemistry to make inferences about tectonic settings or primary rock compositions. As the major rock types within the TVB comprise felsic-intermediate volcanic rocks, it is necessary to first understand the effects that the replacement of primary minerals (predominantly feldspar), and volcanic glass by secondary hydrothermal minerals, have upon chemical element systematics. The most common hydrothermal alteration process affecting the felsic-intermediate volcaniclastic rocks hosting VMS deposits of the southern TVB is replacement of primary feldspar by sericite, effectively resulting in a gain of K from hydrothermal fluids and a loss of Na and Ca from the rock. Additional replacement of feldspars and sericite by chlorite results in an addition of Mg ± Fe to the rocks. Based on the degree of alteration of the samples within this study, it is assumed that the Na, K, Ca, Mg, Fe and SiO_2 have acted as mobile elements. Although other major oxides such as Al_2O_3 and TiO_2 are commonly assumed to be immobile under most alteration conditions (*e.g.*, Barrett and MacLean, 1999), the presence of intense alteration, including locally intense carbonate alteration proximal to massive sulphide horizons, suggests that these elements should be also used with caution. For further discussions on the potential mobility of these elements, as well as other high-field-strength-elements (HFSEs), *see* Pandarinath *et al.* (2008), Jiang *et al.* (2005), Finlow-Bates and Stumpfl (1982), and Hynes (1980). The low-field-strength-elements (*e.g.*, Ba, Rb, Cs, Sr) are considered to be mobile under the alteration conditions in this study, and are not used to discriminate between rock types. The REEs (with the exception of Eu (*e.g.*, Sverjensky, 1984; Whitford *et al.*, 1988)) are generally considered to be immobile except under extreme hydrothermal alteration conditions, when the light REEs may become mobile (Campbell *et al.*, 1984; MacLean and Barrett, 1993).

The coherent behaviour of the heavy REEs in the samples suggest that they were immobile, whereas there are slight shifts in light REE concentrations (especially La) indicating some mobility. The HFSEs, *e.g.*, Zr, Hf, Nb, Ta, Y, Th, are immobile in almost all cases (*e.g.*, Barrett and MacLean, 1999; Lentz, 1999). The coherent behaviour of these elements in the samples suggests that they remained essentially immobile during alteration. The samples analyzed in this study include both volcanic and volcaniclastic rocks. Whereas element immobility can be proven in strictly coherent volcanic facies in the belt, other factors could affect the lithogeochemistry of tuffaceous rocks.

The geochemical data from the three main deposits in the southern TVB, as well as that of the Pats Pond group of Zagorevski *et al.* (2007a) and Rogers (2004), are plotted on an alteration box plot in Figure 4 (Large *et al.*, 2001). This plot uses two common alteration indexes *viz.,* the Hashimoto Alteration Index (AI; Ishikawa *et al.*, 1976) and the chlorite–carbonate–pyrite index (CCPI; Large *et al.*, 2001; *see* Table 3 for formulae). High AI values represent sericite and chlorite alteration products from the breakdown of plagioclase feldspars and volcanic glass; whereas high CCPI values represent chlorite, Fe–Mg carbonates and pyrite alteration typically associated with VMS deposits. Most of the felsic-intermediate rock types that host the VMS deposits at the Tulks Hill, Tulks East and Boomerang deposits are displaced to the right of the 'least altered box', with relatively high AI and CCPI, suggesting that they have been widely affected by hydrothermal activity. For this reason, emphasis is placed on relatively immobile REE and HFSE in the following discussion. In contrast, the data from the Pats Pond group (Zagorevski, 2007a) do not show strong alteration effects as the focus of that study was to sample for geochemical correlations and tectonic discrimination, with altered rocks being avoided.

Tulks East Deposit

The host rocks to the Tulks East deposit are bimodal. The felsic-intermediate (andesitic composition) host rocks are subdivided into crystal tuffs, lapilli tuffs, and rhyolites. Quartz-phyric crystal tuffs dominate both the hanging wall and footwall sequences, and samples from both areas have relatively low Zr/TiO_2 (283 and 272) and Nb/Y ratios (0.07 and 0.03), suggestive of a subalkaline affinity (Table 3; Figure 5). Felsic lapilli tuffs from the hanging wall and footwall have very similar Nb/Y ratios with slightly lower Zr/TiO_2 ratios (201 and 189 respectively), whereas rhyolite from the hanging wall and footwall have similar Zr/TiO_2 but more variable Nb/Y ratios. Quartz–feldspar-phyric crystal tuffs from the hanging wall have a distinctly higher Zr/TiO_2 ratio (809) but with similar Nb/Y ratios. However, the average is skewed by one sample with a high Zr/TiO_2 ratio. The HFSE (*e.g.*, Zr, Hf, Y, Nb and Ta) contents of all the felsic-intermediate rocks are low to moderate, characterizing them as volcanic-arc to ocean-ridge-type rocks on the commonly used HFSE diagrams (Figure 6). Primitive-mantle-normalized plots for the felsic-intermediate rocks (Figures 7 and 8), are characterized by weak to moderate LREE enrichments (with the exception of the footwall felsic tuffs that have a slight depletion), as shown by the La_N/Sm_N ratios in Table 3, slight depletions in MREE causing the slightly concave upward patterns (refer to the Gd_N/Lu_N ratios in Table 3 and Figures 7 and 8), slight to moderate overall REE fractionations, strongly negative Nb and Ti anomalies, variably strong negative Eu anomalies, and slightly positive Zr and Hf anomalies. Most of the felsic-intermediate rocks have very low Zr/Y and La/Yb ratios, similar to published values for tholeiitic rocks (Barrett and MacLean, 1999; Table 3). The Sm/Nd isotopic analyses of two samples of felsic tuff yielded εNd (498 Ma) values of +2.90 and +3.10 (Table 4).

The mafic volcanic rocks from Tulks East are characterized by relatively flat, extended trace-element plots, with values three to four times that of primitive mantle concentrations (Figure 9). Samples display a strong negative Nb anomaly, a slight positive Eu anomaly, and slightly negative Zr and Hf anomalies. The one sample of an andesitic sill has a unique chemistry with a downward concave, extended trace-element profile, similar to that associated with ocean-island or back-arc-basin basalt. On a Ti-V discrimination diagram (after Shervais, 1982), the mafic volcanics plot predominantly in the island-arc tholeiite field, whereas the one sample of an andesitic sill plots in the alkaline field (Figure 10), and on a Th-Zr-Nb plot (after Wood, 1980) the mafic volcanics plot predominantly in the arc-basalt field with the one sample of the andesitic sill plotting at the N-MORB to E-MORB boundary.

Tulks Hill Deposit

The host rocks to the Tulks Hill deposit are also bimodal. Felsic host rocks are dominated by quartz-phyric rhyolite, with minor amounts of quartz-phyric felsic tuff, quartz–feldspar-phyric tuff and lapilli tuff. Rhyolite from the hanging wall and footwall have relatively high average Zr/TiO_2 ratios (928 and 972) and low to moderate Nb/Y average ratios (0.06 and 0.08), suggestive of a subalkaline affinity (Table 3; Figure 5). However, there appears to be at least two subgroups of rhyolite, *viz.,* a group having relatively low HFSE and REE and a group with relatively higher HFSE and REE (*see* Figures 5, 6, and 8; not subdivided for the purposes of Table 3). Using this chemical differentiation, the average Zr/TiO_2 of the enriched group is 1420 ± 100, significantly higher than the other rhyolite. As there is no way to visually or petrographically distinguish these rocks, they have been combined in one group for compari-

Table 3. Summary of some key major- and trace-element ratios for the felsic rocks associated with the VMS deposits in the southern TVB and the Pats Pond group

TULKS EAST STRATIGRAPHY

	Fel. Tuff (HW)		Fel.Tuff (FW)		Fel. Lapilli Tuff		Qtz-fld Tuff (HW)		Rhyolite (HW)		Rhyolite (FW)	
					HW	FW						
	Average	σ	Average	σ	Average	Average	Average	σ	Average	σ	Average	σ
	n = 4, 1		n = 5, 3		n = 1, 1	n = 2, 1	n = 3, 2		n = 2, 2		n = 1, 1	
AI	69.46	31.70	90.06	7.72	46.73	92.29	24.10	17.07	57.58	51.74	92.48	-
CCPI	64.89	22.26	89.99	12.59	53.48	82.66	33.76	14.06	56.75	43.73	75.36	-
Na/K	1.13	1.78	0.25	0.07	0.96	0.21	9.14	10.39	1.99	2.67	0.19	-
Zr/Y	2.23	-	1.99	0.94	1.77	2.52	2.56	1.15	1.15	0.64	1.77	-
Zr/Nb	35.53	4.10	168.41	136.58	38.86	56.18	35.68	2.27	42.83	0.36	39.47	-
Zr/TiO_2	283.11	125.14	272.70	43.37	201.54	189.16	809.10	477.46	298.49	144.60	346.13	-
Zr/Hf	32.34	-	31.81	3.33	30.68	29.37	35.56	2.28	21.64	15.55	30.18	-
Nb/Y	0.07	-	0.03	0.02	0.05	0.04	0.07	0.03	0.03	0.01	0.04	-
Th/Nb	0.35	0.17	2.69	1.54	0.73	1.05	0.91	0.24	1.01	0.30	0.92	-
La_N/Yb_N	1.86	-	0.60	0.53	1.47	1.55	1.53	1.33	1.24	0.15	1.41	-
Ce_N/Yb_N	1.66	-	0.56	0.47	1.37	1.62	1.28	0.99	1.17	0.17	1.31	-
La_N/Th_N	1.39	-	0.31	0.33	0.85	0.60	0.41	0.06	1.02	0.41	0.64	-
La_N/Nb_N	4.50	-	2.96	2.28	5.26	8.10	3.13	1.58	9.27	6.13	5.03	-
Zr_N/Sm_N	0.71	-	1.38	0.62	0.68	0.73	1.17	0.04	0.52	0.35	0.65	-
La_N/Sm_N	1.63	-	0.78	0.63	1.44	1.33	1.68	0.86	1.37	0.01	1.31	-
Gd_N/Lu_N	0.87	-	0.69	0.13	0.89	0.88	0.77	0.19	0.84	0.01	0.87	-
Eu/Eu*	0.30	-	0.61	0.25	1.04	0.33	0.78	0.19	0.74	0.15	0.29	-
Nb/Nb*	0.14	0.16	0.02	0.01	0.04	0.07	0.05	0.02	0.03	0.02	0.04	-
Zr/Zr*	0.19	-	0.28	0.07	0.18	0.20	0.29	0.04	0.13	0.08	0.17	-
Ti/Ti*	0.05	-	0.05	0.02	0.05	0.06	0.02	0.02	0.03	0.03	0.03	-
Nb/Ta	-	-	10.25	6.72	-	-	16.00	-	14.75	14.50	13.00	-

TULKS HILL STRATIGRAPHY

	Fel. Tuff (HW)		Fel.Tuff (FW)		Fel. Lapilli Tuff (HW)		Qtz-fld Tuff (HW)		Rhyolite (HW)		Rhyolite (FW)	
	Average	σ	Average	σ	Average	σ	Average	σ	Average	σ	Average	σ
	n = 2, 0		n = 2, 2		n = 1, 0		n = 1, 1		n = 12, 5		n = 3, 1	
AI	40.10	8.03	57.35	42.44	36.23	-	46.33	-	60.90	31.53	63.72	33.48
CCPI	66.84	10.04	78.93	23.81	34.99	-	27.97	-	51.12	15.30	60.21	23.24
Na/K	3.67	0.42	9.50	13.32	2.56	-	1.16	-	1.82	2.74	3.87	6.31
Zr/Y	-	-	2.22	0.23	-	-	2.44	-	2.14	0.31	2.44	-
Zr/Nb	30.99	7.21	28.35	1.78	36.71	-	29.21	-	35.44	7.01	33.91	10.42
Zr/TiO_2	84.59	5.08	460.09	348.97	1512.82	-	553.00	-	928.21	535.82	972.40	448.61
Zr/Hf	-	-	34.38	0.96	-	-	34.22	-	31.98	1.58	31.32	-
Nb/Y	-	-	0.08	0.00	-	-	0.08	-	0.06	0.01	0.08	-
Th/Nb	0.69	0.23	0.99	0.57	0.80	-	0.95	-	0.92	0.33	0.68	0.43
La_N/Yb_N	-	-	2.39	0.80	-	-	1.82	-	1.48	0.55	1.86	-
Ce_N/Yb_N	-	-	1.93	0.54	-	-	1.53	-	1.31	0.42	1.63	-
La_N/Th_N	-	-	0.63	0.23	-	-	0.45	-	0.65	0.22	0.45	-
La_N/Nb_N	-	-	4.70	1.05	-	-	3.59	-	4.29	0.56	3.94	-
Zr_N/Sm_N	-	-	0.82	0.01	-	-	1.15	-	0.94	0.08	1.02	-
La_N/Sm_N	-	-	2.12	0.36	-	-	2.24	-	1.74	0.34	1.97	-
Gd_N/Lu_N	-	-	0.95	0.11	-	-	0.69	-	0.74	0.13	0.78	-
Eu/Eu*	-	-	0.93	0.23	-	-	0.56	-	0.70	0.15	0.64	-
Nb/Nb*	0.09	0.03	0.04	0.02	-	-	0.04	-	0.06	0.02	0.14	0.14
Zr/Zr*	-	-	0.21	0.00	-	-	0.30	-	0.24	0.02	0.27	-
Ti/Ti*	-	-	0.03	0.02	-	-	0.03	-	0.02	0.01	0.01	-
Nb/Ta	-	-	16.50	-	-	-	-	-	14.83	1.65	15.00	-

Table 3. Continued

	BOOMERANG AND DOMINO STRATIGRAPHY													
	Fel. Tuff (HW)		Fel.Tuff (FW)		Fel. Lapilli Tuff (HW)		Qtz-fld. Tuff (HW)		Qtz-fld. Tuff (FW)		Felsic Sill		Felsic Ashy Tuff	
	Average	σ	Average	σ	Average	σ	Average	σ	Average	σ	Average	σ	Average	σ
	n = 16, 7		n = 4, 3		n = 6, 3		n = 3, 2		n = 3, 2		n = 8, 4		n = 2, 2	
AI	46.21	15.70	59.85	21.60	57.76	10.22	50.65	35.78	55.67	11.43	33.00	8.07	42.61	35.19
CCPI	60.97	9.35	69.64	4.52	55.76	9.09	66.42	23.13	84.63	15.00	44.94	8.28	49.92	17.49
Na/K	16.10	31.64	0.27	0.03	1.33	0.69	8.95	12.15	0.38	0.08	27.39	62.42	9.57	12.78
Zr/Y	2.82	0.75	3.43	0.73	3.67	0.91	2.69	0.14	3.40	0.30	3.73	1.23	5.62	0.63
Zr/Nb	39.66	12.67	29.04	3.47	54.68	15.12	33.45	2.30	39.86	1.52	39.14	6.66	31.04	0.94
Zr/TiO_2	152.65	124.83	156.75	16.14	326.61	217.28	114.50	19.02	193.63	16.82	233.46	140.77	489.33	447.69
Zr/Hf	33.61	2.52	33.92	2.06	38.41	2.88	32.81	0.72	36.51	2.58	35.37	2.20	35.35	0.60
Nb/Y	0.07	0.02	0.11	0.02	0.07	0.03	0.08	0.01	0.09	0.01	0.09	0.03	0.18	0.01
Th/Nb	0.46	0.33	0.41	0.14	0.84	0.46	0.63	0.75	0.31	0.08	0.68	0.40	0.78	0.70
La_N/Yb_N	1.52	0.32	1.83	0.27	2.11	0.37	2.68	1.70	3.50	1.53	2.83	1.63	4.31	1.36
Ce_N/Yb_N	1.49	0.28	1.63	0.25	2.06	0.33	2.38	1.21	3.09	1.59	2.41	1.25	3.60	0.93
La_N/Th_N	1.11	0.55	0.90	0.06	0.84	0.29	1.01	0.50	2.23	0.02	0.96	0.39	0.98	0.54
La_N/Nb_N	3.43	1.22	2.60	0.29	5.80	1.96	5.44	4.22	6.09	2.17	4.72	0.83	4.84	2.22
Zr_N/Sm_N	1.05	0.27	1.41	0.10	1.20	0.29	0.83	0.21	0.97	0.36	1.21	0.22	1.18	0.11
La_N/Sm_N	1.38	0.32	1.89	0.09	1.73	0.23	1.86	0.94	2.22	0.09	2.14	0.69	2.82	0.98
Gd_N/Lu_N	0.97	0.17	0.84	0.06	0.98	0.08	1.03	0.02	1.13	0.51	1.05	0.27	0.94	0.27
Eu/Eu*	0.89	0.10	0.83	0.13	0.88	0.06	1.03	0.12	1.40	0.36	0.90	0.04	0.88	0.10
Nb/Nb*	0.15	0.10	0.09	0.01	0.07	0.04	0.16	0.15	0.11	0.08	0.10	0.10	0.06	0.04
Zr/Zr*	0.28	0.07	0.37	0.04	0.33	0.08	0.23	0.04	0.27	0.09	0.32	0.07	0.36	0.01
Ti/Ti*	0.13	0.05	0.12	0.01	0.04	0.02	0.09	0.01	0.08	0.03	0.10	0.02	0.07	0.06
Nb/Ta	19.64	8.33	13.94	2.58	17.50	5.07	14.75	2.47	10.50	0.71	12.54	4.71	13.08	2.24

	PATS POND GROUP STRATIGRAPHY											
	PP1		PP2		PP3		PP4		PP5		PP6	
	Average	σ	Average	σ	Average	σ	Average	σ	Average	σ	Average	σ
	n = 4, 4		n = 2, 2		n = 5, 5		n = 7, 7		n = 1, 1		n = 2, 2	
AI	43.25	6.42	39.20	5.13	31.65	9.64	30.90	10.83	42.51	-	7.16	3.15
CCPI	63.01	9.31	87.01	3.00	54.18	16.81	40.17	10.32	50.32	-	4.60	0.00
Na/K	44.07	40.98	25.90	22.06	71.10	69.59	13.41	11.94	2.69	-	98.56	113.29
Zr/Y	2.24	0.21	2.30	0.28	2.05	0.38	2.01	0.64	2.17	-	2.69	0.68
Zr/Nb	43.14	9.08	23.42	1.30	40.52	8.33	45.61	5.55	37.01	-	32.11	0.16
Zr/TiO_2	57.31	7.13	33.92	0.59	96.93	37.73	139.72	40.15	44.60	-	764.12	171.80
Zr/Hf	34.34	3.00	32.44	0.27	31.25	1.96	31.69	2.50	32.64	-	33.24	0.96
Nb/Y	0.05	0.02	0.10	0.02	0.05	0.01	0.05	0.02	0.06	-	0.08	0.02
Th/Nb	2.62	1.16	1.67	0.09	1.27	0.31	1.40	0.39	0.40	-	1.07	0.20
La_N/Yb_N	3.20	0.96	3.63	0.49	1.50	0.23	1.22	0.34	0.67	-	1.32	0.22
Ce_N/Yb_N	2.86	0.81	2.98	0.44	1.33	0.20	1.06	0.29	0.69	-	1.20	0.13
La_N/Th_N	0.44	0.09	0.44	0.00	0.44	0.10	0.44	0.16	0.58	-	0.29	0.04
La_N/Nb_N	9.01	2.39	6.30	0.35	4.66	1.12	4.90	1.15	1.99	-	2.56	0.11
Zr_N/Sm_N	0.55	0.05	0.57	0.01	0.85	0.17	0.87	0.19	0.99	-	1.54	0.06
La_N/Sm_N	1.78	0.15	2.40	0.04	1.56	0.48	1.45	0.22	0.84	-	1.94	0.17
Gd_N/Lu_N	1.33	0.13	1.06	0.15	0.86	0.13	0.68	0.07	0.86	-	0.66	0.01
Eu/Eu*	0.92	0.06	1.16	0.13	0.99	0.31	0.68	0.12	1.08	-	0.47	0.01
Nb/Nb*	0.02	0.01	0.02	0.00	0.03	0.01	0.03	0.00	0.09	-	0.04	0.01
Zr/Zr*	0.16	0.01	0.16	0.00	0.21	0.04	0.22	0.05	0.24	-	0.37	0.03
Ti/Ti*	0.14	0.02	0.24	0.01	0.13	0.04	0.09	0.03	0.27	-	0.03	0.00
Nb/Ta	5.32	1.16	-	-	-	-	-	-	5.11	-	11.78	2.17

AI= Hashimoto index = 100*[(MgO+K_2O)/(MgO+K_2O+Na_2O+CaO)] (Ishikawa *et al.,* 1976)
CCPI = chlorite-carbonate-pyrite index = 100*[(MgO+FeO*0/(MgO+FeO*+K_2O+Na_2O)] (Large *et al.,* 2001)
Na/K = Na_2O/K_2O
samples normalized to primitive mantle (values after Sun and McDonough, 1989)
Eu/Eu* = Eupm/(Gdpm*Smpm)0.5, Nb/Nb* = 0.5*Nbpm/(Thpm+Lapm), Zr/Zr* = 0.5*Zrpm/(Gdpm + Smpm), Ti/Ti* = 0.5*Tipm/(Gdpm + Smpm)
pm = primitive mantle normalized
n= number of samples analyzed for (major-element analysis, trace-element and REE alalysis)

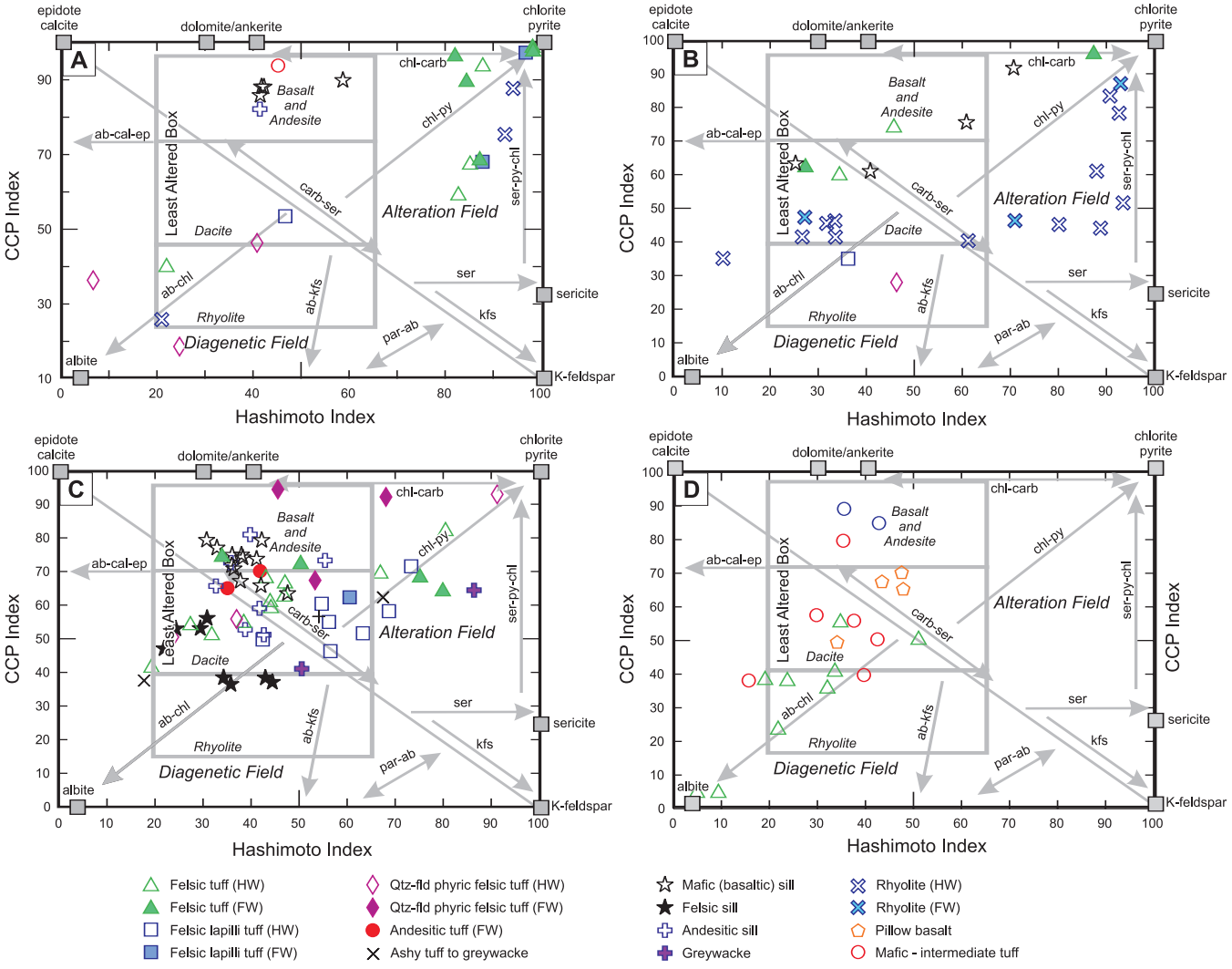

Figure 4. *Alteration box plots of Large* et al. *(2001), with vectors for various alteration minerals and alteration versus diagenetic fields. CCP index = chlorite–carbonate–pyrite index. A) = Tulks East deposit, B) = Tulks Hill deposit, C) = Boomerang deposit, D) Pats Pond group. AI= Hashimoto index = 100*[(MgO+K_2O)/(MgO+K_2O+Na_2O+CaO)] (Ishikawa* et al.*, 1976), CCPI = chlorite–carbonate–pyrite index = 100*[(MgO+FeO)/(MgO+FeO+K_2O+Na_2O)] (Large* et al.*, 2001).*

son purposes. Felsic tuffs, from the hanging wall and footwall, have much lower Zr/TiO_2 averages (84 and 460) compared to the rhyolite, and have similar Nb/Y ratios. Although not analyzed for REEs, a sample of a quartz–feldspar-phyric tuff from the hanging wall of the deposit also has very high Zr/TiO_2 (1512), similar to the subset of rhyolite described above. The HFSE (*e.g.*, Zr, Hf, Y, Nb, Ta) contents of all the felsic-intermediate rocks are low to moderate, characterizing them as volcanic-arc to ocean-ridge-type rocks on commonly used HFSE diagrams (Figure 6). Primitive-mantle-normalized plots for the felsic-intermediate rocks are characterized by moderate to strong LREE enrichments (*see* the La_N/Sm_N ratios in Table 3 and Figures 7 and 8), slight depletions in MREE causing the slightly concave upward patterns (refer to the Gd_N/Lu_N rations in Table 3 and Figures 7 and 8), moderate overall REE fractionations, strongly negative Nb and Ti anomalies, slightly negative Eu anomalies, and approximately flat Zr and Hf. Most all of the felsic-intermediate rocks have very low Zr/Y and La/Yb ratios, similar to published values for tholeiitic rocks (Barrett and MacLean, 1999; Table 3). The Sm/Nd isotopic composition analysis of two samples of felsic tuff yielded εNd (498 Ma) values of +2.99 and +3.02 (Table 4).

The mafic volcanics from Tulks Hill are characterized by weak to moderately fractionated extended trace-element plots, with values four to ten times that of primitive mantle concentrations (Figure 9). Samples display a strong negative Nb anomaly, a strong negative Ti anomaly in two of the four samples, a slightly positive Eu anomaly, and negative Zr and Hf anomalies. As such, the samples appear as two groups with calc-alkaline basalt to island-arc tholeiite signatures.

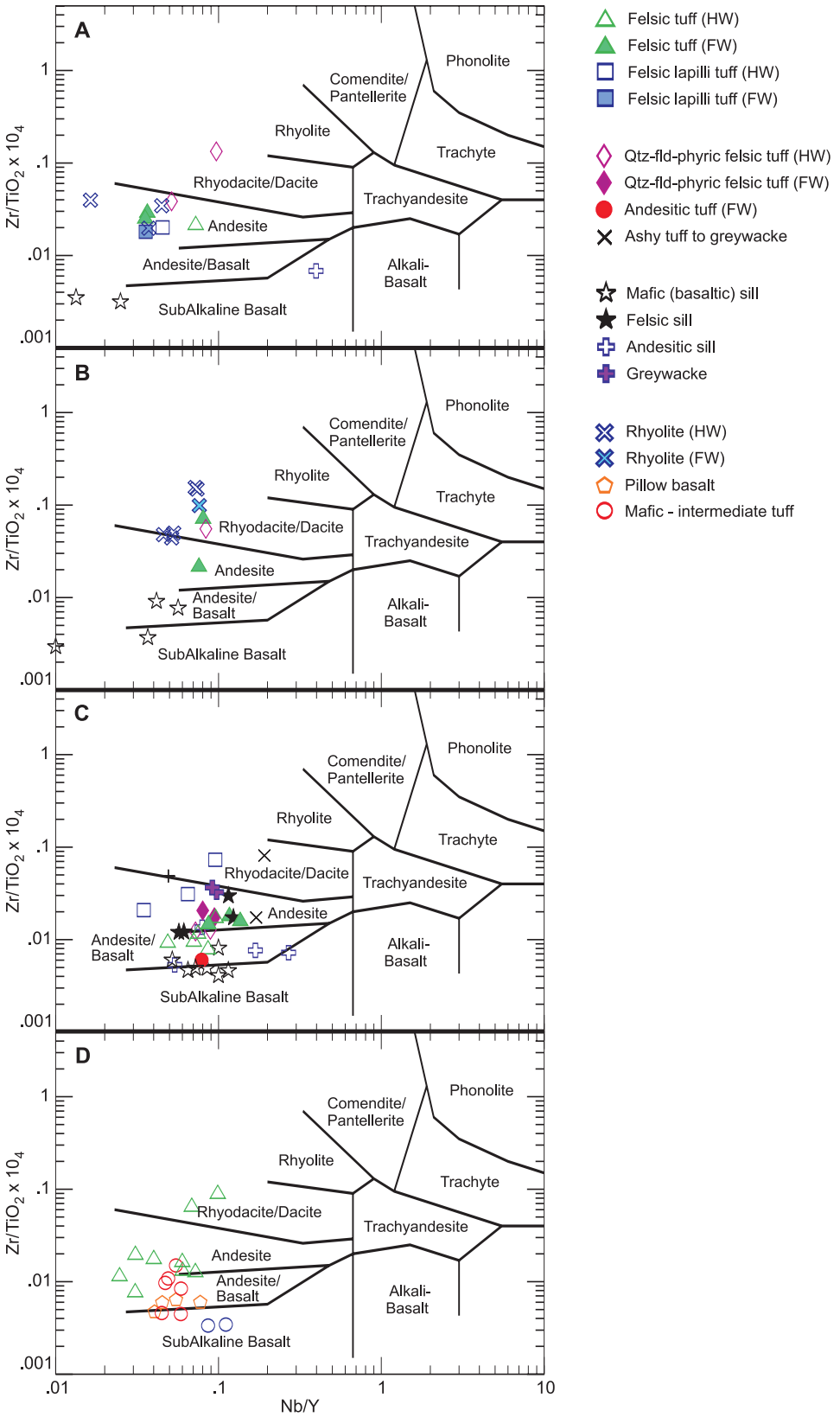

Figure 5. *Nb/Y versus Zr/TiO$_2$ rock type classification diagram (Winchester and Floyd, 1977). A) Tulks East deposit, B) Tulks Hill deposit, C) Boomerang deposit, D) Pats Pond group. Pats Pond group chemistry from Rogers (2004) and Zagorevski* et al. *(2007a).*

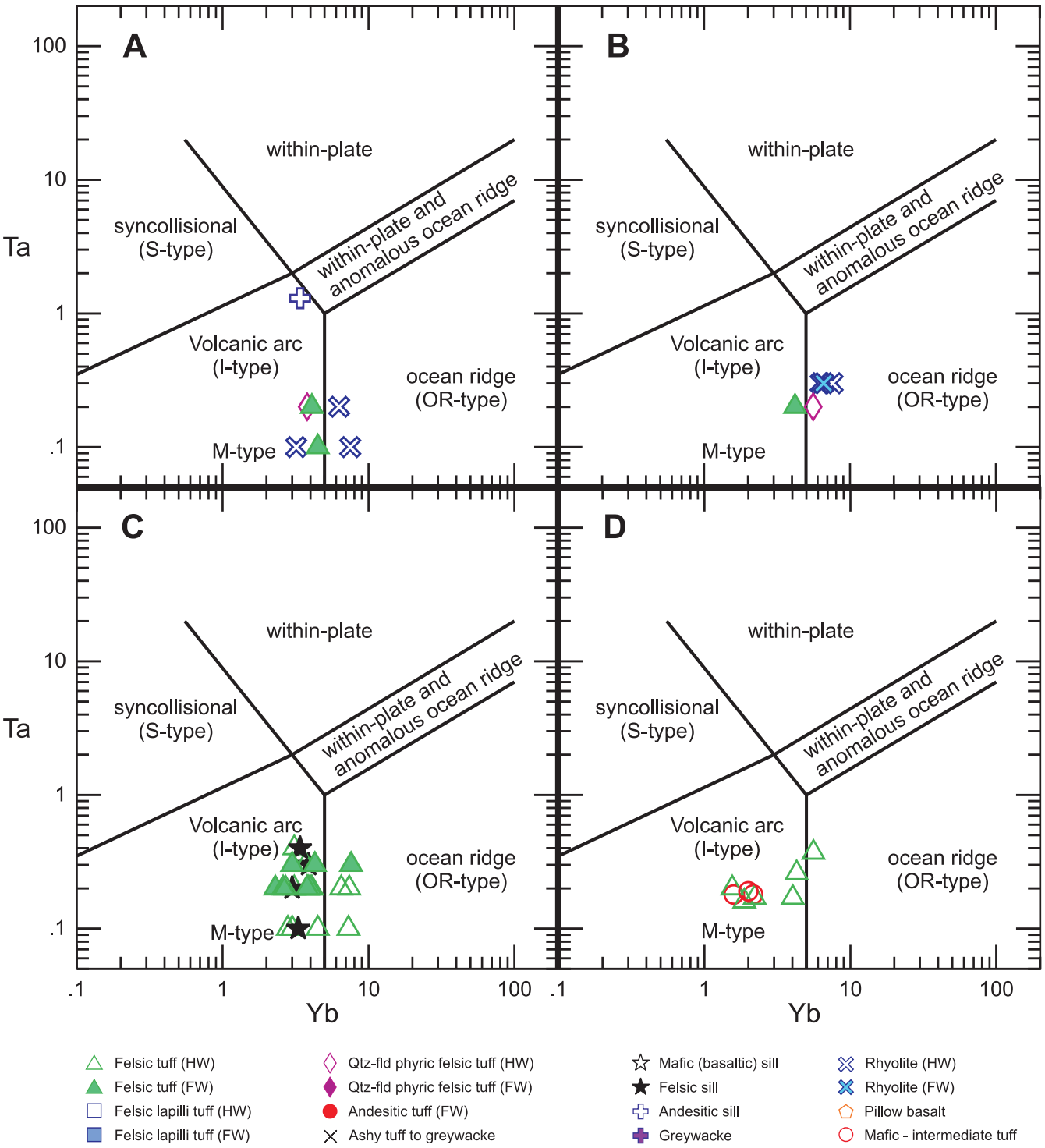

Figure 6. *Yb versus Ta (Pearce* et al.*, 1984) discrimination diagrams for the host felsic volcanic rocks of the three main VMS deposits in the southern Tulks Volcanic Belt and the Pats Pond group. A) Tulks East deposit, B) Tulks Hill deposit, C) Boomerang deposit, D) Pats Pond group. Pats Pond group chemistry from Rogers (2004) and Zagorevski* et al. *(2007a).*

On a Ti-V discrimination diagram, the two mafic volcanic samples, with the island-arc tholeiite signature, plot in the same field, whereas those with calc-alkaline basalt signatures contain very little V and plot toward the bottom of the diagram (Figure 10), and on a Th-Zr-Nb plot (after Wood, 1980) all of the mafic volcanic samples plot in the arc-basalt field.

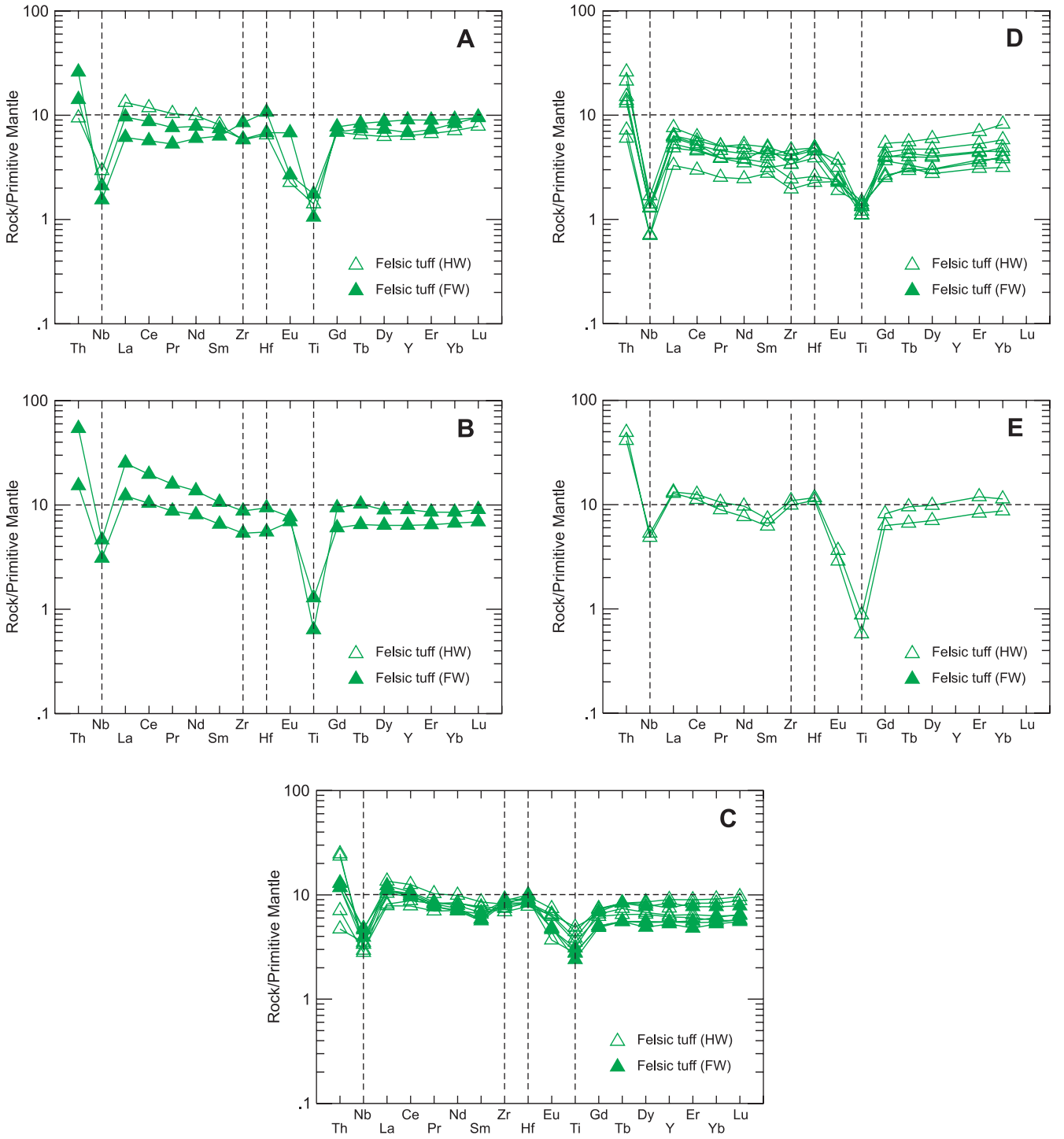

Figure 7. *Primitive-mantle-normalized trace-element plots for the southern Tulks Volcanic Belt and Pats Pond group felsic tuff rocks. Note that in 7A to 7C, these rocks host the massive sulphide deposits. A). Tulks East deposit, B) Tulks Hill deposit, C) Boomerang deposit, D) Pats Pond 4 (PP4), E) Pats Pond 6 (PP6). Pats Pond group chemistry from Rogers (2004) and Zagorevski* et al. *(2007a). Primitive mantle values from Sun and McDonough (1989).*

Boomerang Deposit

Host rocks to the Boomerang deposit appear to form a continuum from mafic through to felsic-intermediate compositions. However, the andesitic sills illustrated in Figure 5 have different chemical characteristics and may not be genetically associated with the host rocks to the deposit. If these are excluded, the data have a bimodal distribution. The

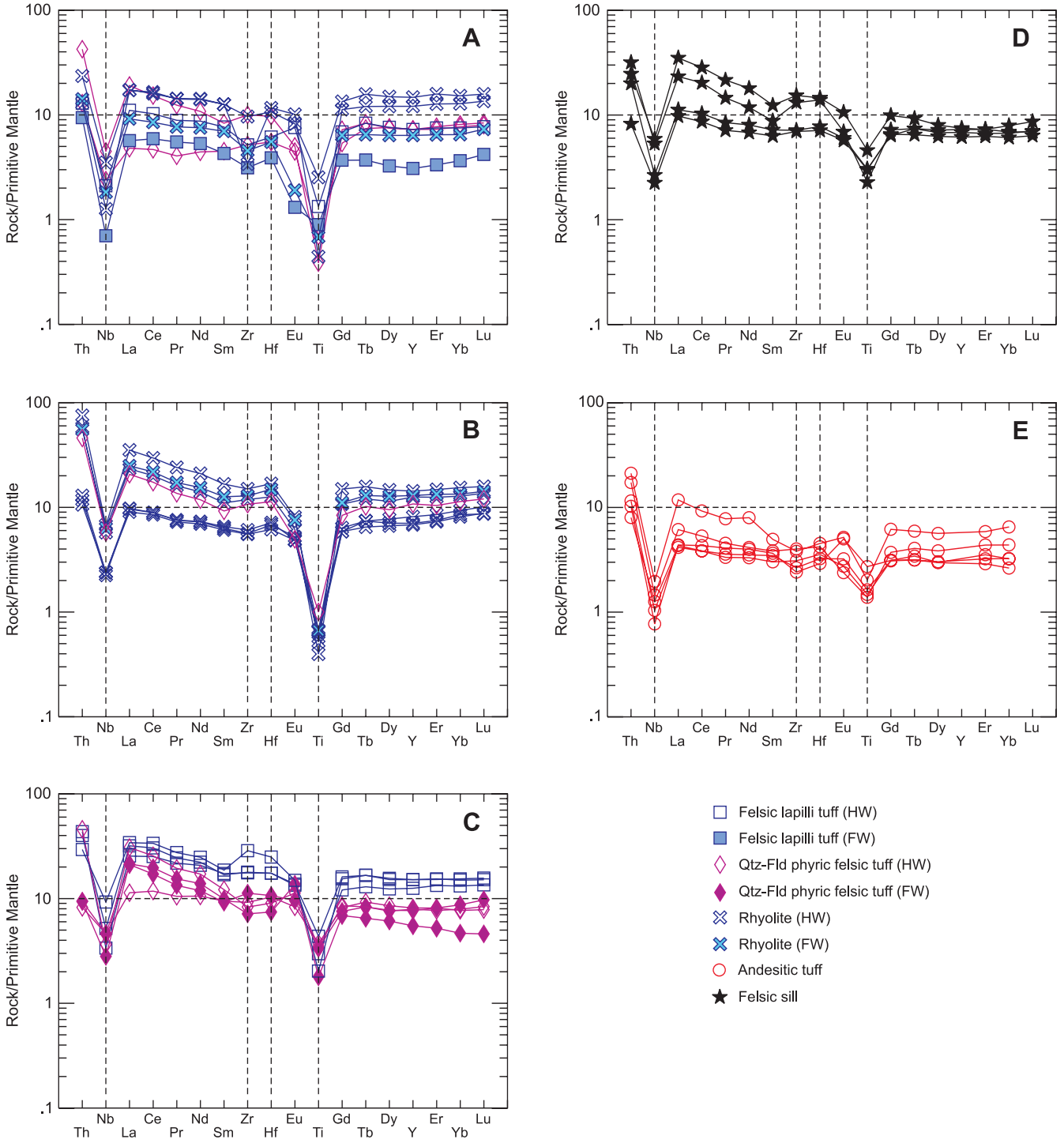

Figure 8. *Primitive-mantle-normalized trace-element plots for other felsic to intermediate rocks from the southern Tulks Volcanic Belt and Pats Pond group. A). Tulks East deposit, B) Tulks Hill deposit, C) Boomerang deposit, D) Boomerang deposit, E) Pats Pond 3 (PP3). Pats Pond group chemistry from Rogers (2004) and Zagorevski* et al. *(2007a). Primitive mantle values from Sun and McDonough (1989).*

felsic-intermediate rocks have much lower Zr/TiO_2 ratios than those associated with the Tulks Hill deposit, and more closely resemble data from Tulks East (Figure 5). Felsic-intermediate host rocks are dominated by quartz-phyric tuff that have average Zr/TiO_2 ratios of 152 and 156, and average Nb/Y ratios of 0.07 and 0.11 in the hanging wall and footwall, respectively. Quartz–feldspar-phyric tuffs in the hanging wall and footwall have very similar ratios, whereas

Table 4. Sm/Nd isotopic data

Sample	Deposit or Unit	Sm	Nd	$^{147}Sm/^{144}Nd$ (measured)	143/144 (measured)	Age (Ma)	143/144 initial	eNd CHUR (T)c	Model Age T(DM) ***DePaolo
JHC-06-022	Tulks East (TE-99-04)	1.30	4.32	0.1815	0.512737	498	0.512144905	2.90	1434.15
JHC-06-003	Tulks East (TE-94-01)	2.30	8.13	0.1707	0.512712	498	0.512155137	3.10	1171.48
JHC-06-057	Tulks Hill (T-192)	3.59	14.18	0.1529	0.512648	498	0.512149205	2.99	996.05
JHC-06-043	Tulks Hill (T-197)	4.92	19.21	0.1548	0.512656	498	0.512151007	3.02	1006.93
JHC-06-172	Domino (GA-97-05)	6.52	27.86	0.1416	0.512669	491	0.512213572	4.07	803.39
JHC-06-184	Domino (GA-97-05)	2.37	8.59	0.1669	0.512759	491	0.512222199	4.24	934.87
JHC-06-229	Boomerang (GA-04-11)	3.46	10.74	0.1949	0.512902	491	0.512275143	5.27	1137.49
JHC-06-236	Boomerang (GA-04-11)	2.48	9.39	0.1596	0.512786	491	0.512272678	5.22	743.80
VL02A246b	PP6	2.87	11.22	0.1546	0.512701	488	0.512206803	3.86	892.49
VL02A221	PP4	0.85	3.12	0.1655	0.512777	488	0.51224796	4.66	855.56
VL02A128	PP4	0.63	2.17	0.1766	0.512854	488	0.512289477	5.47	799.11
VL02A202	PP1	2.68	10.14	0.1598	0.512493	488	0.51198218	-0.53	1547.64
VL02A026	PP1	3.30	13.04	0.153	0.512515	488	0.512025917	0.33	1322.16

** T DM = Nd depleted mantle model age - calculated using the Goldstein 143/144 0.513163; and 147/144 of 0.2137
calulated using present day chondritic uniform reservoir with $^{143}Nd/^{144}Nd = 0.512638$ & $^{147}Sm/^{144}Nd = 0.1967$
***TDM Depaolo - calculated using the two stage evolution of Depaolo, 1981
(143/144) is adjusted from the deviation to JNdi-1 Standard (0.512115), mean measured value of the standard gives 0.512135 +- 9 (2sigma StdDev)
Pats Pond data (PP6, PP4, and PP1) from Zagorevski *et al.,* 2007a.

lapilli tuffs in the hanging wall, ash-rich tuffs, and felsic sills have higher Zr/TiO_2 ratios of 326, 489 and 233 respectively (Table 3). The HFSE (Zr, Hf, Y, Nb, Ta) contents of all the felsic-intermediate rocks are low to moderate, characterizing them as volcanic-arc to ocean-ridge type rocks on commonly used HFSE diagrams (Figure 6). Primitive-mantle-normalized plots for the felsic-intermediate rocks are characterized by weak to moderate LREE enrichments (refer to the La_N/Sm_N ratios in Table 3 and Figures 7 and 8), flat MREE patterns that have only very minor local depletions, weak to moderate overall REE fractionation, weak to moderate negative Nb and Ti anomalies, slightly negative Eu anomalies, and prominent positive Zr and Hf anomalies for the felsic-intermediate tuffs, lapilli tuffs, and some felsic sills (Figures 7 and 8). Most of the felsic-intermediate rocks have very low Zr/Y and La/Yb ratios, similar to published values for tholeiitic rocks (Barrett and MacLean, 1999; Table 3). The Sm/Nd isotopic composition analysis of four samples of felsic-intermediate tuff from the Boomerang and nearby Domino deposits yielded εNd (491 Ma) values from +4.07 to +5.27 (Table 4).

The mafic volcanic rocks from Boomerang are characterized by weak LREE-enriched to flat extended trace-element plots, with values four to ten times that of primitive mantle concentrations. These characteristics are very similar to the profile for N-MORB (Figure 9). Samples display a moderately positive Th anomaly and a moderately negative Nb anomaly. As such, the samples have island-arc tholeiite signatures. In contrast, samples of the andesitic sills have much higher concentrations of HFSE and REE, display higher degrees of REE fractionation, and have variably moderate to strong negative Nb and Ti anomalies. These features are suggestive of transitional calc-alkaline basalt to island-arc tholeiite signatures (Figure 9). On a Ti-V discrimination diagram, the mafic volcanic samples plot predominantly within the island-arc tholeiite field but are transitional into the MORB field, whereas the andesitic sills predominantly plot within the alkaline field (Figure 10), and on a Th-Zr-Nb plot (*after* Wood, 1980) the mafic volcanics plot predominantly in the arc-basalt field with one sample of the andesitic sill plotting in the N-MORB field.

Pats Pond Group

As mentioned earlier, the Pats Pond group, as defined by Zagorevski *et al.* (2007a), has been subdivided into six stratigraphic subunits. For the purposes of this report, the chemistry will be discussed based on rock type, consistent with the previous descriptions of deposit geochemistry.

Felsic-intermediate rocks of the Pats Pond group are hosted within the PP4 and PP6 subunits. Subunit PP4 consists of quartz ± feldspar, felsic-intermediate tuffs, and is characterized by relatively low Zr/TiO_2 (139) and Nb/Y (0.05) ratios, placing the samples in the subalkaline andesitic field (Figure 5). The HFSE (Zr, Hf, Y, Nb, Ta) contents of all the felsic-intermediate rocks are low to moderate, characterizing them as volcanic-arc rocks on commonly used HFSE diagrams (Figure 6). Primitive-mantle-normalized plots for subunit PP4 are characterized by moderate LREE enrichments (refer to the La_N/Sm_N ratios in Table 3 and Figures 7 and 8), moderate depletion of MREE, weak overall REE fractionations, moderate to strong negative Nb and Ti anomalies, slightly negative Eu anomalies, and negligible Zr and Hf anomalies (Figure 7). Subunit PP4 has low

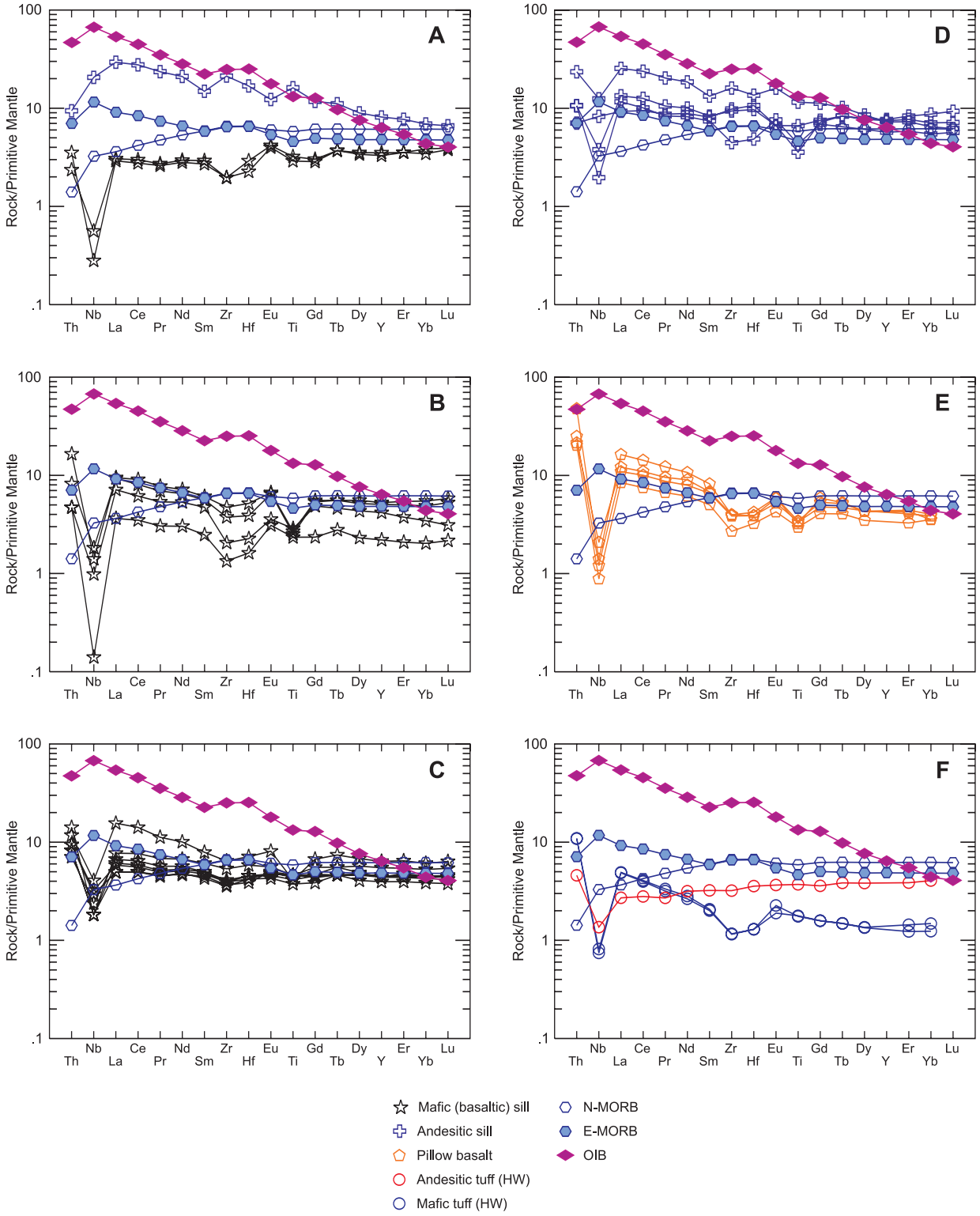

Figure 9. *Primitive-mantle-normalized trace-element plots for mafic to intermediate volcanics of the southern Tulks Volcanic Belt and Pats Pond group rocks. A) Tulks East deposit basalt and andesite, B) Tulks Hill deposit basaltic sills, C) Boomerang deposit basaltic sills, D) Boomerang deposit andesitic sills, E) Pats Pond group (PP1) basalt, F) PP2 mafic tuff and PP5 intermediate tuff. Pats Pond group chemistry from Rogers (2004) and Zagorevski* et al. *(2007a). Shown for comparison are N-MORB, E-MORB and OIB. Primitive mantle values, and N-MORB, E-MORB and OIB values from Sun and McDonough (1989). N-MORB = mid-ocean-ridge basalt, E-MORB = enriched mid-ocean-ridge basalt, OIB = ocean-island basalt.*

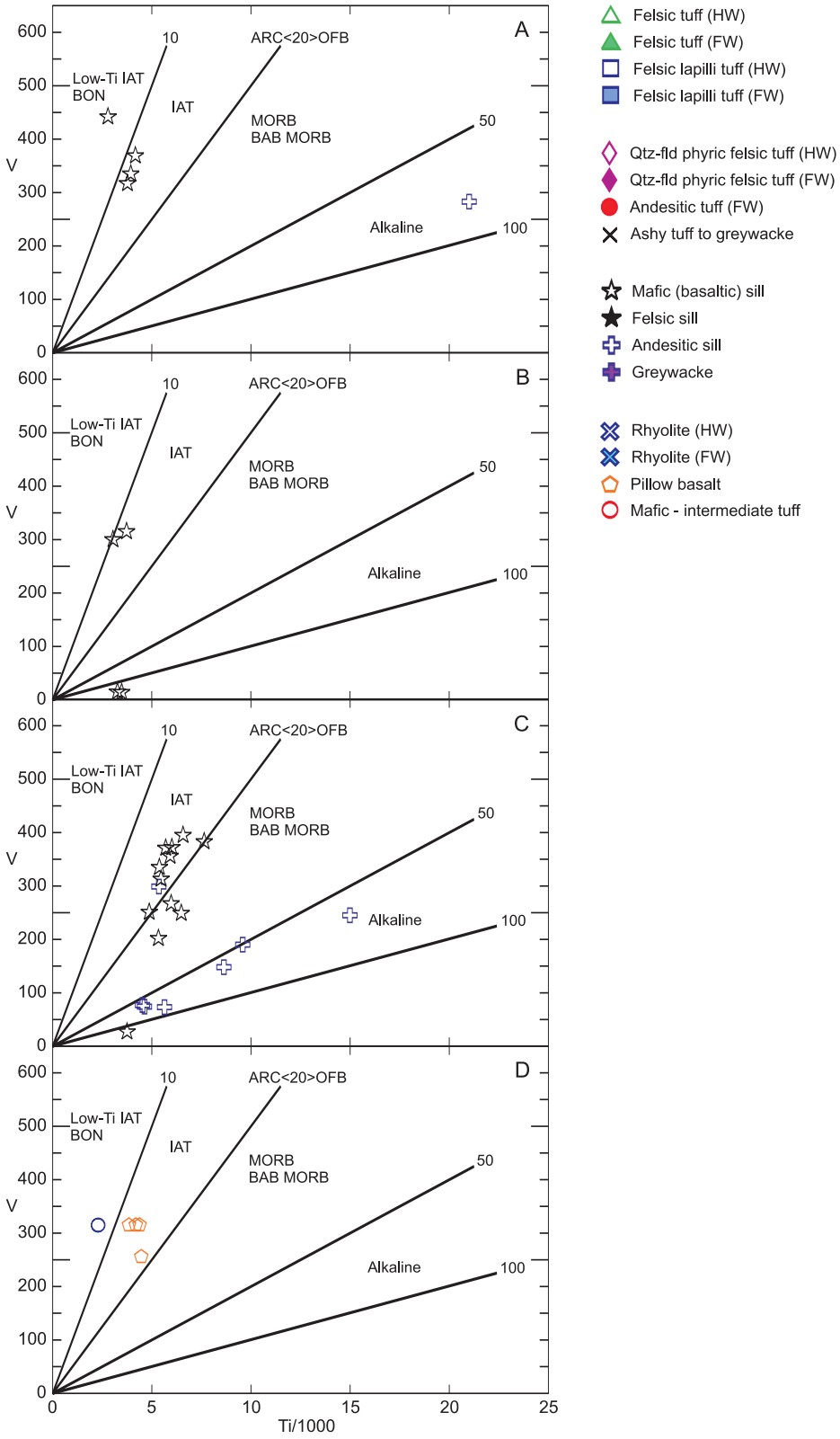

Figure 10. *Ti-V (Shervais, 1982) discrimination plot for mafic rocks of the southern Tulks Volcanic Belt and Pats Pond group. A) Tulks East deposit, B) Tulks Hill deposit, C) Boomerang deposit, D) Pats Pond group. Pats Pond group chemistry from Rogers (2004) and Zagorevski* et al. *(2007a). BON = boninite, IAT = island-arc tholeiite, MORB = mid-ocean-ridge basalt, BABB = back-arc-basin basalt.*

Zr/Y and La/Yb ratios, similar to published values for tholeiitic rocks (Barrett and MacLean, 1999; Table 3). Two Sm/Nd isotopic composition analysis yielded εNd (487 Ma) values of +4.7 and +5.5 (Table 4).

Subunit PP6 consists of high-silica trondhjemitic rhyolite. Compared to subunit PP4, it displays much higher Zr/TiO_2 ratios with similar Nb/Y (Figure 5). The HFSE (Zr, Hf, Y, Nb, Ta) contents of these rocks are low to moderate, plotting on the boundary of volcanic-arc and ocean-ridge-type rocks on commonly used HFSE diagrams (Figure 6). Primitive-mantle-normalized plots for subunit PP6 are characterized by moderate LREE enrichments (refer to the La_N/Sm_N ratios in Table 3 and Figure 7), moderate depletion of MREE, weak overall REE fractionations, moderate to strong negative Nb and Ti anomalies, negative Eu anomalies, and prominent positive Zr and Hf anomalies (Figure 7). A Sm/Nd isotopic composition analysis yielded εNd (487 Ma) of +3.86 (Table 4).

Intermediate andesitic tuff comprises subunit PP3 and a sample from this unit was used to date the Pats Pond group (Zagorevski *et al.*, 2007a). These rocks consist of feldspar ± quartz, felsic-intermediate tuffs and have very similar chemical characteristics to subunit PP4 (*see* Figures 7 and 8).

Mafic to intermediate volcanic rocks of the Pats Pond group consist of subunits PP1, PP2 and PP5 of Zagorevski *et al.* (2007a). Subunit PP1 consists of transitional calc-alkaline basaltic andesite to island-arc tholeiite where the mafic volcanic rocks have strong, enriched LREE's, strong Th enrichment, prominent negative Nb anomalies, slight negative Ti anomalies, and negative Zr and Hf anomalies (Figure 9). Andesitic sills have much higher concentrations of HFSE and REE, display higher degrees of REE fractionation, and have variably moderate to strong negative Nb and Ti anomalies; suggestive of transitional calc-alkaline basalt to island-arc tholeiite signatures. On a Ti-V discrimination diagram, the mafic volcanic samples plot predominantly within the island-arc tholeiite field (Figure 10), and on a Th-Zr-Nb plot (*after* Wood, 1980) the mafic volcanics all plot in the arc-basalt field. The Sm/Nd isotopic composition analysis of two samples of subunit PP1 yielded εNd (487 Ma) values from +0.33 to -0.53 (Table 4).

Subunit PP2 consists of calc-alkaline basalt and mafic tuffs. This subunit displays very similar chemistry to the PP1 rocks, with the exception that it has overall lower abundances of HFSE and REE and it lacks the negative Ti anomaly (Figure 9). Subunit PP5 consists of an intermediate to mafic tuff and has chemical characteristics very similar to the mafic volcanic rocks of the Boomerang deposit. This unit has fairly flat to weak depleted LREE, with overall flat extended trace-element patterns, and values two to three times that of primitive mantle concentrations. The chemical profile parallels that for N-MORB; although with lower element concentrations. The unit displays a moderately positive Th anomaly and a moderately negative Nb anomaly, and as such has an island-arc tholeiite signature.

DISCUSSION

This study was begun to attempt to decipher lithological packages that host VMS mineralization in the southern Tulks Volcanic Belt, in hopes of aiding exploration. The U–Pb geochronological data and geochemical data presented in this paper lead to five main conclusions. First, the new U–Pb results show that the volcanic rocks included within the TVB actually include felsic rock sequences of at least two ages, *i.e.*, 498 +6/-4 Ma and 491 ± 3 Ma. As a first-order conclusion, this supports the proposal that the southern Tulks Belt is composed of westward-younging volcanic rocks (*e.g.*, van Staal *et al.*, 2005; Zagorevski *et al.*, 2007a). However, the ages from Tulks Hill and Boomerang deposits overlap in error at their respective lower and upper limits, so the results do not preclude an interpretation, in which there is a continuum of volcanism over several million years, rather than having discrete sequences. Second, the ages from both Boomerang and Tulks Hill deposits constrain the timing of VMS mineralization and suggest that there was more than one mineralization event in this area. This is particularly true if we assume the age on the porphyry at Tulks Hill represents a minimum age for mineralization. Third, that the age from the felsic sill at the Boomerang deposit is identical to the host sequence confirms that bimodal volcanism was synchronous with mineralization, as previously proposed by Hinchey (2006) based on textural relationships. Fourth, zircon inheritance from the Boomerang deposit samples suggest that, in part, these rocks developed on a substrate of older (Cambrian) rocks possibly equivalent to other parts of the VLSG, such as the Tally Pond group (*e.g.*, McNicoll *et al.*, 2008; *cf.* Zagorevski *et al.*, 2007a). Finally, the variations in the felsic and mafic rock types and their geochemical and isotopic signatures, suggest that these sequences probably developed in a complex environment of episodic arc development and rifting. These five points are discussed in more detail below.

AGES OF VOLCANISM AND MINERALIZATION

The identical ages of 491 ± 3 Ma obtained for the felsic tuff that hosts the massive-sulphide mineralization at Boomerang, and a crosscutting felsic dyke, closely constrain the timing of mineralization. The age is younger than the 498 +6/-4 Ma age obtained on a subvolcanic porphyry at the Tulks Hill deposit (Evans *et al.*, 1990), although their error envelopes do overlap at their respective older and younger limits. If the revised age of 496.5 ± 1 Ma for Tulks Hill is used (G.R. Dunning, personal communication, 2008), there is no overlap between these ages.

The age of 491 ± 3 Ma obtained for the Boomerang deposit is slightly older than the 487 ± 3 Ma age reported for the Pats Pond group (Zagorevski *et al.*, 2007a). However, these ages overlap extensively at their older and younger limits, respectively.

There is no simple interpretation of these data, but the closer correspondence of the ages from the Boomerang deposit and the Pats Pond group suggests that a link between these sequences is more likely than a link between Boomerang and the Tulks deposits. The alternative interpretation is that all of these subdivisions of the VLSG represent nothing more than a long-lived period of volcanism and sedimentation that extended from *ca.* 498 to *ca.* 487 Ma, a period of some 11 Ma.

The identical ages obtained for the felsic dyke and the volcaniclastic felsic host tuff at the Boomerang deposit have implications for the environment of VMS mineralization. The presence of such synchronous sills, both felsic and mafic, is characteristic of high-temperature extensional regimes such as those found in rifted-arc environments. The high heat flow in such settings leads to the formation of hydrothermal convection cells and VMS-style mineralization at or below the seafloor (*e.g.*, Franklin *et al.*, 2005; Galley *et al.*, 2007). A rifted-arc environment is also favoured by the variable chemical signatures of the felsic and mafic rocks at Boomerang, as discussed below.

ZIRCON INHERITANCE PATTERNS

The SHRIMP data presented herein indicate zircon inheritance of ca. 510 and 514 Ma from the felsic sill sample and inheritance of ca. 530 Ma from the felsic tuff sample. The inheritance ages from the felsic sill are similar to the crystallization ages of volcanic rocks previously dated at the Duck Pond deposit, within the Tally Pond group (McNicoll *et al.*, 2008, and references therein). These data suggest that the host rocks to the Boomerang deposit formed on a substrate represented by these older rocks, rather than being juxtaposed at a later time. The *ca.* 530-Ma inherited zircon from the felsic tuff could represent an older volcanic source. Zagorevski (2007a) documented inheritance of *ca.* 560 Ma from the Pats Pond group, and Squires and Moore (2004) and McNicoll *et al.* (2008) documented inheritance of *ca.* 565 Ma and 573 Ma zircons within felsic rocks of the Tally Pond group, suggesting that these rocks were built on a Precambrian substrate. The development of the VLSG thus appears to have been a sequential process of arc magmatism, in which arcs were built on older continental basement, rather than in an ensimatic environment (*cf.* Rogers *et al.*, 2006 and Zagorevski *et al.*, 2007a).

LITHOGEOCHEMICAL PATTERNS

The detailed geochemistry provided in this report provides information on the tectonic settings of felsic and mafic rocks associated with VMS mineral deposits and also allows comparison of these host sequences.

The relatively low HFSE and REE concentrations of the rocks, coupled with the ubiquitous, yet variably developed, negative Nb and Ti anomalies on primitive-mantle-normalized, extended trace-element plots for the felsic and intermediate rocks are diagnostic of formation in an arc environment (*e.g.*, Pearce and Peate, 1995). In light of the zircon inheritance, it could be argued that the negative Nb and Ti anomalies in the felsic rocks could be due to re-melting of older crustal source material with arc parentage. However, the synchronous mafic rocks of calc-alkaline and island-arc tholeiitic affinity suggests overall development in an arc environment.

A comparison of the felsic-intermediate host rocks from the four areas illustrates some subtle but potentially important differences. First, rhyolites from the Tulks Hill deposit have elevated Zr/TiO_2 ratios compared to the rocks from other areas. However, in this case, the variation in the Zr/TiO_2 ratios is predominantly related to lower TiO_2 rather than variation in HFSE concentrations, and this pattern is most likely indicative of greater fractionation in the Tulks Hill deposit rhyolites. It should be noted that the felsic tuffs from the Tulks Hill deposit have Zr/TiO_2 ratios similar to those of felsic tuffs and rhyolites from other areas.

Additional chemical variations in the felsic-intermediate volcanic rocks occur in the degree of LREE enrichment and the extent of the negative Nb and Ti anomalies, which appear to be correlated. Tulks Hill deposit samples appear to have greater LREE enrichment and larger and more pronounced negative Nb and Ti anomalies compared to the Boomerang deposit samples, whereas the Tulks East deposit samples have similar LREE enrichment and similar, but slightly larger, overall Nb and Ti anomalies. The Boomerang felsic-intermediate rocks have extended trace-element patterns similar to the PP4 grouping from the Pats Pond group, and positive Zr and Hf anomalies similar to the PP6 grouping. The mafic volcanic rocks throughout the belt vary from transitional calc-alkaline basalts to island-arc tholeiites at Tulks Hill, Boomerang and in the Pats Pond group. This conclusion is dependant upon the assumption that the andesitic sills at the Boomerang deposit are the same age as the other volcanic rocks. In contrast, the mafic volcanic rocks at Tulks East deposit and true mafic sills at the Boomerang deposit are characterized by island-arc tholeiitic

signatures. The mixtures of calc-alkaline and tholeiitic sequences are best explained by the progressive rifting of predominantly calc-alkaline arcs (*cf.* Zagorevski *et al.*, 2007a). The variations in the chemistry of felsic and intermediate rocks may also reflect this general process.

The last chemical variation that is observed between the four areas is differences in εNd of the felsic rocks. The Boomerang deposit and Pats Pond group felsic-intermediate samples have higher εNd (+4 to +5.5) compared to those from the Tulks Hill and Tulks East deposits (εNd of around +3). Although there is no easy interpretation of these data, the apparent bimodal grouping suggests that the Boomerang area is more similar to the Pats Pond group than either the Tulks Hill or Tulks East deposits. However, it should be noted that felsic-intermediate rocks similar to those that host the Tulks Hill and Tulks East deposits locally contain eNd signatures of around +4 to +5.0 (*e.g.*, Rogers, 2004; Hinchey, J. unpublished data) adding to the ambiguity of such data.

CONCLUSIONS

New U–Pb zircon data, isotopic data, and geochemical data from volcanic rocks in the southern TVB of the VLSG are not simple to interpret. In conjunction with previous data, the results suggest that VMS mineralization at the Boomerang deposit is resolvably younger than that at the Tulks Hill deposit. However, the ages are closer to those obtained elsewhere in that part of the unit defined as the Pats Pond group. Subtle lithogeochemical variations, and higher εNd signatures for felsic-intermediate samples from the Boomerang deposit and the Pats Pond group also appear to support this correlation. Inherited zircon of *ca.* 530–510 Ma suggests that the host rocks at Boomerang were deposited upon a substrate of older rocks including material of similar age to the Tally Pond group and, perhaps, also Precambrian basement.

Follow-up research, including additional lithogeochemical, isotopic and geochronological studies, has been initiated to characterize the host rocks to VMS deposits in the northern part of the TVB. Results will hopefully aid in further unravelling the complexities in the TVB.

ACKNOWLEDGMENTS

The geochronological work summarized in this article was conducted at the GSC geochronology laboratory. The laboratory staff are thanked for their assistance with sample processing and analysis. Staff of Messina Minerals Inc. and Prominex Resources Corp. are thanked for granting access to company drillcores and data, and for many informative discussions. This report was reviewed by Andy Kerr, Lawson Dickson and Alex Zagorevski, who are thanked for many useful comments that helped improve the scientific merit of this paper.

REFERENCES

Barbour, D.M. and Thurlow, J.G.
1982: Case histories of two massive sulphide discoveries in central Newfoundland. *In* Prospecting in Areas of Glaciated Terrain. *Edited by* P. Davenport. Canadian Institute of Mining, Metallurgy and Petroleum, pages 300-320.

Barrett, T.J. and MacLean, W.H.
1999: Volcanic sequences, lithogeochemistry and hydrothermal alteration in some bimodal volcanic-associated massive sulphide systems. *In* Volcanic-Associated Massive Sulfide Deposits: Processes and Examples in Modern and Ancient Settings. *Edited by* C.T. Barrie and M.D. Hannington. Reviews in Economic Geology, Society of Economic Geologists, Volume 8, pages 101-127.

Campbell, I.H., Lesher, C.M., Coad, P., Franklin, J.M., Gorton, M.P. and Thurston, P.C.
1984: Rare-earth element mobility in alteration pipes below massive Cu-Zn sulphide deposits. Chemical Geology, Volume 45, pages 181-202.

Colman Sadd, S.P., Dunning, G.R. and Dec, T.
1992: Dunnage-Gander relationships and Ordovician orogeny in central Newfoundland: a sediment provenance and U/Pb age study. American Journal of Science, Volume 292, pages 317-355.

Dearin, C.
2006: Technical Report on the Tulks South Property. Map staked licences: 11924M, 11925M and Reid Lot 228. Red Indian Lake area, central Newfoundland, Canada. NTS 12A/06 and 12A/11, 158 pages.

Dunning, G.R., Kean, B.F., Thurlow, J.G. and Swinden, H.S.
1987: Geochronology of the Buchans, Roberts Arm, and Victoria Lake groups and Mansfield Cove Complex, Newfoundland. Canadian Journal of Earth Sciences, Volume 24, pages 1175-1184.

Dunning, G.R., Swinden, H.S., Kean, B.F., Evans, D.T.W. and Jenner, G.A.
1991: A Cambrian island arc in Iapetus: Geochronology and geochemistry of the Lake Ambrose volcanic belt, Newfoundland Appalachians. Geological Magazine, Volume 128, pages 1-17.

Evans, D.T.W. and Kean, B.F.
2002: The Victoria Lake Supergroup, central Newfoundland – its definition, setting and volcanogenic massive sulphide mineralization. Newfoundland Department of Mines and Energy, Geological Survey, Open File NFLD/2790, 68 pages.

Evans, D.T.W., Kean, B.F. and Dunning, G.R.
1990: Geological studies, Victoria Lake Group, central Newfoundland. *In* Current Research. Newfoundland Department of Mines and Energy, Geological Survey Branch, Report 90-1, pages 131-144.

Finch, C.J.
1998: Inductively coupled plasma – emission spectrometry (ICP-ES) at the geochemical laboratory. *In* Current Research. Newfoundland Department of Mines and Energy, Geological Survey Branch, Report 98-1, pages 179-194.

Finlow-Bates, T. and Stumpfl, E.F.
1981: The behaviour of so-called immobile elements in hydrothermally altered rocks associated with volcanogenic submarine-exhalative ore deposits. Mineralium Deposita, Volume 16, pages 319-328.

Franklin, J.M., Gibson, H.L., Jonasson, I.R. and Galley, A.G.
2005: Volcanogenic massive sulfide deposits. *In* 100th Anniversary Volume, 1905-2005. Economic Geology, pages 523-560.

Galley, A.G., Hannington, M.D. and Jonasson, I.R.
2007: Volcanogenic massive sulphide deposits. *In* Mineral Deposits of Canada: A Synthesis of Major Deposit Types, District Metallogeny, the Evolution of Geological Provinces, and Exploration Methods. *Edited by* W.D. Goodfellow. Geological Association of Canada, St. John's, NL, Canada. Special Publication No. 5, pages 141-162.

Hinchey, J.G.
2007: Volcanogenic massive sulphides of the Southern Tulks Volcanic Belt, central Newfoundland: Preliminary findings and overview of styles and environments of mineralization. *In* Current Research. Newfoundland and Labrador Department of Natural Resources, Geological Survey, Report 07-1, pages 117-143.

2008: Volcanogenic massive sulphides of the Northern Tulks Volcanic Belt, central Newfoundland: Preliminary findings, overview of deposit reclassifications and mineralizing environments. *In* Current Research. Newfoundland and Labrador Department of Natural Resources, Geological Survey, Report 08-1, pages 151-172.

Hynes, A.
1980: Carbonatization and mobility of Ti, Y, and Zr in Ascot Formation metabasalts, SE Quebec. Contributions to Mineralogy and Petrology, Volume 75, pages 79-87.

Ishikawa, Y., Sawaguchi, T., Ywaya, S. and Horiuchi, M.
1976: Delineation of prospecting targets for Kuroko deposits based on modes of volcanism of underlying dacite and alteration haloes. Mining Geology, Volume 26, pages 105-117.

Jambor, J.L. and Barbour, D.M.
1987: Geology and mineralogy of the Tulks pyritic massive sulphide deposit. *In* Buchans Geology, Newfoundland. *Edited by* R.V. Kirkham. Geological Survey of Canada, Paper 86-24, pages 219-226.

Jiang, S.-Y., Wang, R.-C., Xu, X.-S. and Zhao, K.-D.
2005: Mobility of high field strength elements (HFSE) in magmatic-, metamorphic-, and submarine-hydrothermal systems. Physics and Chemistry of the Earth, Volume 30, pages 1020-1029.

Kean, B.F.
1977: Geology of the Victoria Lake map area (12A/06), Newfoundland. Newfoundland Department of Mines and Energy, Mineral Development Division, Report 77-4, 11 pages.

Kean, B.F., Dean, P.L. and Strong, D.F.
1981: Regional geology of the Central Volcanic Belt of Newfoundland. Geological Association of Canada, Special Paper 22.

Kean, B.F. and Evans, D.T.W
1986: Metallogeny of the Tulks Hill volcanics, Victoria Lake Group, central Newfoundland. *In* Current Research. Newfoundland Department of Mines and Energy, Mineral Development Division, Report 86-1, pages 51-57.

Krogh, T.E.
1982: Improved accuracy of U-Pb ages by creation of more concordant systems using an air abrasion technique. Geochimica et Cosmochimica Acta, Volume 46, pages 637-649.

Large, R.R., Gemmell, J.B., Paulick, H. and Huston, D.L.
2001: The alteration box plot: A simple approach to understanding the relationship between alteration mineralogy and lithogeochemistry associated with volcanic-hosted massive sulphide deposits. Economic Geology, Volume 96, pages 957-971.

Lentz, D.R.
1999: Petrology, geochemistry, and oxygen isotope interpretation of felsic volcanic and related rocks hosting the Brunswick 6 and 12 massive sulphide deposits (Brunswick Belt), Bathurst mining camp, New Brunswick, Canada. Economic Geology, Volume 94, pages 57-86.

Lissenberg, C.J., Zagorevski, A., Rogers, N., van Staal, C.R. and Whalen, J.B.
2005: Geology, Star Lake, Newfoundland and Labrador. Geological Survey of Canada, Open File 1669, scale 1:50 000.

Ludwig, K.R.
1998: On the treatment of concordant uranium-lead ages. Geochimica et Cosmochimica Acta, Volume 62, pages 665-676.

2003: User's manual for Isoplot/Ex rev. 3.00: A Geochronological Toolkit for Microsoft Excel. Special Publication, 4, Berkeley Geochronology Center, Berkeley, 70 pages.

MacLean, W.H. and Barrett, T.J.
1993: Lithogeochemical techniques using immobile elements. Journal of Geochemical Exploration, Volume 48, pages 109-133.

McKenzie, C., Desnoyers, D., Barbour, D. and Graves, M.
1993: Contrasting volcanic-hosted massive sulphide styles in the Tulks Belt, central Newfoundland. Exploration and Mining Geology, Volume 2, Number 1, pages 73-84.

McNicoll, V.J., Squires, G. , Kerr, A. and Moore, P.
2008: Geological and metallogenic implications of new U-Pb zircon geochronological data from the Tally Pond volcanic belt, central Newfoundland. *In* Current Research. Newfoundland and Labrador Department of Natural Resources, Geological Survey, Report 08-1, pages 1-19.

Moreton, C.
1984: A geological, geochemical, and structural analysis of the Lower Ordovician Tulks Hill Cu-Zn- (Pb) volcanogenic massive sulphide deposit, central Newfoundland, Canada. M.Sc. thesis, Memorial University of Newfoundland, St. John's, 320 pages.

Noranda
1998: Precious and base metal properties available for option in central Newfoundland. Summary Report, ca. 500 pages.

Pandarinath, K., Dulski, P., Torres-Alvarada, I.S. and Verma, S.P.
2008: Element mobility during the hydrothermal alteration of rhyolitic rocks of the Los Azufres geothermal field, Mexico. Geothermics, Volume 37, pages 53-72.

Parrish, R.R., Roddick, J.C., Loveridge, W.D. and Sullivan, R.W.
1987: Uranium-lead analytical techniques at the Geochronology Labroratory, Geological Survey of Canada. *In* Radiogenic Age and Isotope Studies, Report 1. Geological Survey of Canada, Paper 87-2, pages 3-7.

Pearce, J.A., Harris, N.B.W. and Tindle, A.G.
1984: Trace element discrimination diagrams for the tectonic interpretation of granitic rocks. Journal of Petrology, Volume 25, pages 956-983.

Pearce, J.A. and Peate, D.W.
1995: Tectonic implications of the composition of volcanic arc magmas. Annual Reviews in Earth and Planetary Science. Volume 23, pages 251-285.

Roddick, J.C.
1987: Generalized numerical error analysis with applications to geochronology and thermodynamics. Geochimica et Cosmochimica Acta, Volume 51, pages 2129-2135.

Rogers, N.
2004: Geochemical database, Red Indian Line project, central Newfoundland. Geological Survey of Canada, Open File 4605, 1 CD-ROM.

Rogers, N., van Staal, C.R., McNicoll, V.J., Squires, G.C., Pollock, J. and Zagorevski, A.
2005: Geology, Lake Ambrose and part of Buchans, Newfoundland and Labrador. Geological Survey of Canada, Open File 4544, scale 1: 50 000.

Rogers, N., van Staal, C.R., McNicoll, V.J., Pollock, J., Zagorevski, A. and Whalen, J.B.
2006: Neoproterozoic and Cambrian arc magmatism along the eastern margin of the Victoria Lake Supergroup: A remnant of Ganderian basement in central Newfoundland? Precambrian Research, Volume 147, pages 320-341.

Rollinson, H.
1993: Using geochemical data: evaluation, presentation, interpretation. Longman, Harlow, 352 pages.

Saunders, P.
1999: Report on the Tulks property, Newfoundland. J.

Tuach Geological Consultants Inc. Newfoundland and Labrador Geological Survey, Assessment file 12A/11/0883, 1999, 17 pages.

Shervais, J.W.
1982: Ti-V plots and the petrogenesis of modern and ophiolitic lavas. Earth and Planetary Science Letters, Volume 59, pages 101-118.

Squires, G.C.
2008: The Boomerang and Duck Pond VMS deposits, Newfoundland: Birth by "raining" or "stewing"? Geological Association of Canada – Newfoundland and Labrador Section Annual Spring Technical Meeting, February, 2008, Program with Abstracts, page 29.

Squires, G.C.S. and Moore, P.J.
2004: Volcanogenic massive sulphide environments of the Tally Pond volcanics and adjacent areas: Geological, lithogeochemical and geochronological results. *In* Current Research. Newfoundland and Labrador Department of Natural Resources, Geological Survey, Report 04-1, pages 63-91.

Squires, G., Tallman, P., Sparkes, K., Hyde, D., House, F. and Regular, K.
2005a: Messina Minerals Inc.'s Boomerang Deposit (or, a fitting reward for doggedly coming back to the same property). GAC Newfoundland Section, Fall Field Trip for 2005, pages 14-16.

2005b: Messina Minerals' new Boomerang VMS discovery: Preliminary evaluation of a sub-seafloor replacement-style massive sulphide deposit. CIMM Newfoundland Branch Meeting, November, 2005, Program with Abstracts, page 15.

2006: Messina Minerals' Boomerang and Domino discoveries: An update. Unpublished Department of Natural Resources Winter Seminar Series.

Stern, R.A.
1997: The GSC Sensitive High Resolution Ion Microprobe (SHRIMP): analytical techniques of zircon U-Th-Pb age determinations and performance evaluation. *In* Radiogenic Age and Isotopic Studies, Report 10. Geological Survey of Canada, Current Research 1997-F, pages 1-31.

Stern, R.A. and Amelin, Y.
2003: Assessment of errors in SIMS zircon U-Pb geochronology using a natural zircon standard and NIST SRM 610 glass. Chemical Geology, Volume 197, pages 111-142.

Sun, S.S. and McDonough, W.F.
1989: Chemical and isotopic systematics of ocean basalts: Implications for mantle composition and processes. Geological Society Special Publication 42, pages 313-345.

Sverjensky, D.A.
1984: Europium redox equilibria in aqueous solutions. Earth and Planetary Science Letters, Volume 67, pages 70-78.

Swinden, H.S.
1990: Regional geology and metallogeny of central Newfoundland. *In* Metallogenic Framework of Base and Precious Metal Deposits, Central and Western Newfoundland. *Edited by* H.S. Swinden, D.T.W. Evans and B.F. Kean. Eight IAGOD Symposium Field Trip Guidebook. Geological Survey of Canada, Open File 2156, pages 1-27.

Swinden, H.S., Jenner, G.A., Kean, B.F. and Evans, D.T.W.
1989: Volcanic rock geochemistry as a guide for massive sulphide exploration in central Newfoundland. *In* Current Research. Newfoundland Department of Mines, Geological Survey Branch, Report 89-1, pages 201-219.

van Staal, C.R., Dewey, J.F., Mac Niocaill, C. and McKerrow, W.S.
1998: The Cambrian - Silurian tectonic evolution of the northern Appalachians and British Caledonides: history of a complex west- and southwest-Pacific type segment of Iapetus. Geological Society, London, Special Publication 143, pages 199-242.

van Staal, C.R., Valverde-Varuero, P., Zagorevski, A., Rogers, N., Lissenberg, C.J. and McNicoll, V.J.
2005: Geology, Victoria Lake, Newfoundland and Labrador. Geological Survey of Canada, Open File 1667, scale 1:50 000.

Whitford, D.J., Korsch, M.J., Porritt, P.M. and Craven, S.J.
1988: Rare earth element mobility around the volcanogenic polymetallic massive sulphide deposit at Que River, Tasmania, Australia. Chemical Geology, Volume 68, pages 105-119.

Williams, H.
1995: Geology of the Appalachian-Caledonian Orogen in Canada and Greenland. Geological Survey of Canada, Geology of Canada: Temporal and Spatial Divisions, Chapter 2, pages 21-44.

Williams, H., Colman-Sadd, S.P. and Swinden, H.S.
1988: Tectono-stratigraphic subdivisions of central Newfoundland. *In* Current Research, Part B. Geological Survey of Canada, Paper 88-1B, pages 91-98.

Winchester, J.A. and Floyd, P.A.
1977: Geochemical discrimination of different magma series and their differentiation products using immobile elements. Chemical Geology, Volume 20, pages 325-343.

Wood, D.A.
1980: The application of a Th-Hf-Ta diagram to problems of tectonmagmatic classification and to establishing the nature of crustal contamination of basaltic lavas of the British Tertiary volcanic province. Earth and Planetary Science Letters, Volume 50, pages 11-30.

York, D.
1969: Least squares fitting of a straight line with correlated errors. Earth and Planetary Science Letters, Volume 5, pages 320-324.

Zagorevski, A., van Staal, C.R., McNicoll, V. and Rogers, N.
2007a: Upper Cambrian to Upper Ordovician peri-Gondwanan island arc activity in the Victoria Lake Supergroup, central Newfoundland: Tectonic development of the northern Ganderian margin. American Journal of Science, Volume 307, pages 339-370.

Zagorevski, A., van Staal, C.R. and McNicoll, V.
2007b: Distinct Taconic, Salinic, and Acadian deformation along the Iapetus suture zone, Newfoundland Appalachians. Canadian Journal of Earth Sciences, Volume 44, pages 1567-1585.

Zagorevski, A., van Staal, C. R., McNicoll, V., Rogers, N. and Valverde-Vaquero, P.
2008: Tectonic architecture of an arc-arc collision zone, Newfoundland Appalachians. *In* Formation and Applications of the Sedimentary Record in Arc Collision Zones. *Edited by* A. Draut, P.D. Clift and D.W. Scholl. Pages 309-334.